Westinghouse Energy Systems

WCAP-12431

ANALYSIS OF CAPSULE U FROM THE COMMONWEALTH EDISON COMPANY BYRON UNIT 2 REACTOR VESSEL RADIATION SURVEILLANCE PROGRAM

E. Terek
E. P. Lippincott
L. Albertin

October 1989

Work Performed Under Shop Order BFHP-106

Prepared by Westinghouse Electric Corporation
for the Commonwealth Edison Company

Approved by: T. A. Meyer
T. A. Meyer, Manager
Structural Materials and Reliability Technology

WESTINGHOUSE ELECTRIC CORPORATION
Nuclear and Advanced Technology Division
P.O. Box 2728
Pittsburgh, Pennsylvania 15230-2728

PREFACE

This report has been technically reviewed and verified.

Reviewer

Sections 1 through 5, 7, and 8	N. K. Ray
Section 6	E. P. Lippincott

TABLE OF CONTENTS

LIST OF ILLUSTRATIONS

LIST OF ILLUSTRATIONS (Cont)

LIST OF TABLES

LIST OF TABLES (Cont)

LIST OF TABLES (Cont)

SECTION 1.0
SUMMARY OF RESULTS

The analysis of the reactor vessel material contained in surveillance Capsule U, the first capsule to be removed from the Commonwealth Edison Company Byron Unit 2 reactor pressure vessel, led to the following conclusions:

- The capsule received an average fast neutron fluence (E > 1.0 MeV) of 3.96×10^{18} n/cm^2 after 1.15 EFPY of plant operation.

- Irradiation of the reactor vessel lower shell forging MK24-3 Charpy specimens to 3.96×10^{18} n/cm^2 (E > 1.0 MeV) resulted in no 30 and 50 ft-lb transition temperature increases for specimens oriented parallel to the major working direction (tangential orientation) and a 25°F transition temperature increase for specimens oriented normal to the major working direction (axial orientation).

- The weld metal and weld HAZ metal Charpy specimens irradiated to 3.96×10^{18} n/cm^2 (E > 1.0 MeV) resulted in 30 and 50 ft-lb transition temperature increases of 0 and 25°F, respectively. This results in a 30 ft-lb transition temperature of -65°F and a 50 ft-lb transition temperature of 0°F for the weld metal and a 30 ft-lb transition temperature of -145°F and a 50 ft-lb transition temperature of -125°F for the HAZ metal.

- The average upper shelf energy of the shell forging MK24-3 showed no decrease in energy after irradiation to 3.96×10^{18} n/cm^2 (E > 1.0 MeV). The weld metal showed no decrease in upper shelf energy after irradiation to 3.96×10^{18} n/cm^2 (E > 1.0 MeV). Both materials exhibit a more than adequate upper shelf energy level for continued safe plant operation and are expected to maintain an upper shelf energy of no less than 50 ft-lb throughout the life of the vessel as required by 10CFR50, Appendix G.

- The surveillance capsule test results do not indicate any significant changes in the RT_{NDT} values projected for the reactor vessel.

- The calculated end-of-life (32 EFPY) maximum neutron fluence (E > 1.0 MeV) for the Byron Unit 2 reactor vessel is as follows:

  Vessel inner radius - 3.03×10^{19} n/cm^2
  Vessel 1/4 thickness - 1.66×10^{19} n/cm^2
  Vessel 3/4 thickness - 3.57×10^{18} n/cm^2

SECTION 2.0
INTRODUCTION

This report presents the results of the examination of Capsule U, the first capsule to be removed from the reactor in the continuing surveillance program which monitors the effects of neutron irradiation on the Byron Unit 2 reactor pressure vessel materials under actual operating conditions.

The surveillance program for the Byron Unit 2 reactor pressure vessel materials was designed and recommended by the Westinghouse Electric Corporation. A description of the surveillance program and the preirradiation mechanical properties of the reactor vessel materials are presented by L. R. Singer.[1] The surveillance program was planned to cover the 40-year design life of the reactor pressure vessel and was based on ASTM E-185-79, "Standard Practice for conducting Surveillance Tests for light-water cooled Nuclear Power Reactor Vessels". Westinghouse Power Systems personnel were contracted to aid in the preparation of procedures for removing capsule "U" from the reactor and its shipment to the Westinghouse Science and Technology Center where the postirradiation mechanical testing of the Charpy V-notch impact and tensile surveillance specimens were performed at the remote metallographic facility.

This report summarized the testing of and the postirradiation data obtained from surveillance Capsule "U" removed from the Byron Unit 2 reactor vessel and discusses the analysis of these data.

SECTION 3.0
BACKGROUND

The ability of the large steel pressure vessel containing the reactor core and its primary coolant to resist fracture constitutes an important factor in ensuring safety in the nuclear industry. The beltline region of the reactor pressure vessel is the most critical region of the vessel because it is subjected to significant fast neutron bombardment. The overall effects of fast neutron irradiation on the mechanical properties of low alloy, ferritic pressure vessel steels such as SA 508 Class 2 (base material of the Commonwealth Edison Company Station Byron Unit 2 reactor pressure vessel lower shell forging) are well documented in the literature. Generally, low alloy ferritic materials show an increase in hardness and tensile properties and a decrease in ductility and toughness under certain conditions of irradiation.

A method for performing analyses to guard against fast fracture in reactor pressure vessels have been presented in "Protection Against Nonductile Failure," Appendix G to Section III of the ASME Boiler and Pressure Vessel Code. The method uses fracture mechanics concepts and is based on the reference nil-ductility temperature (RT_{NDT}).

RT_{NDT} is defined as the greater of either the drop weight nil-ductility transition temperature (NDTT per ASTM E-208) or the temperature 60°F less than the 50 ft-lb (and 35-mil lateral expansion) temperature as determined from Charpy specimens oriented normal (transverse) to the major working direction of the material. The RT_{NDT} of a given material is used to index that material to a reference stress intensity factor curve (K_{IR} curve) which appears in Appendix G of the ASME Code. The K_{IR} curve is a lower bound of dynamic, crack arrest, and static fracture toughness results obtained from several heats of pressure vessel steel. When a given material is indexed to the K_{IR} curve, allowable stress intensity factors can be obtained for this material as a function of temperature. Allowable operating limits can then be determined using these allowable stress intensity factors.

RT_{NDT} and, in turn, the operating limits of nuclear power plants can be adjusted to account for the effects of radiation on the reactor vessel material properties. The radiation embrittlement changes in mechanical properties of a given reactor pressure vessel steel can be monitored by a reactor surveillance program such as the Byron Unit 2 Reactor Vessel Radiation Surveillance Program,[1] in which a surveillance capsule is periodically removed from the operating nuclear reactor and the encapsulated specimens are tested. The increase in the average Charpy V-notch 30 ft-lb temperature (ΔRT_{NDT}) due to irradiation is added to the original RT_{NDT} to adjust the RT_{NDT} for radiation embrittlement. This adjusted RT_{NDT} (RT_{NDT} initial + ΔRT_{NDT}) is used to index the material to the K_{IR} curve and, in turn, to set operating limits for the nuclear power plant which take into account the effects of irradiation on the reactor vessel materials.

SECTION 4.0
DESCRIPTION OF PROGRAM

Six surveillance capsules for monitoring the effects of neutron exposure on the Byron Unit 2 reactor pressure vessel core region material were inserted in the reactor vessel prior to initial plant startup. The six capsules were positioned in the reactor vessel between the neutron shield pads and the vessel wall as shown in figure 4-1. The vertical center of the capsules is opposite the vertical center of the core.

Capsule U was removed after 1.15 effective full power years of plant operation. This capsule contained Charpy V-notch, tensile, and 1/2 T compact tension (CT) specimens (figure 4-2) from the intermediate shell forging MK24-3 and submerged arc weld metal representative of the intermediate to lower shell beltline weld seam of the reactor vessel and Charpy V-notch specimens from weld heat-affected zone (HAZ) material. All heat-affected zone specimens were obtained from within the HAZ of forging MK24-3 of the representative weld.

The chemical composition, heat treatment and touchness data of the surveliiance material are presented in Tables 4-1 through 4-4. The chemical analyses reported in Table 4-1 were obtained from unirradiated material used in tne surveliiance program. In addition, a chemical analysis using Inductively Coupled Plasma Spectrometry (ICPS) was performed on irradiated specimens from forging MK24-3 and weld metal and is reported in Table 4-2. The chemistry results from the NBS certified reference standards are reported in Table 4-3. Table 4-4 contains the toughness data for the reactor vessel materials.

All test specimens were machined from the 1/4 thickness location of the forging. Test specimens represent material taken at least one forging thickness from the quenched end of the forging. Base metal Charpy V-notch impact and tension specimens were oriented with the longitudinal axis of the

specimen parallel to the major working direction of the forging (tangential orientation) and also normal to the major working direction (axial orientation). Charpy V-notch and tensile specimens from the weld metal were oriented with the longitudinal axis of the specimens transverse to the welding direction. The CT specimens in the Capsule U were machined such that the simulated crack in the specimen would propagate normal and parallel to the major working direction for the forging specimen and parallel to the weld direction.

Capsule U contained dosimeter wires of pure copper, iron, nickel, and aluminum-0.15% colbalt (cadmium-shielded and unshielded). In addition, cadmium shielded dosimeters of neptunium (Np^{237}) and uranium (U^{238}) were contained in the capsule.

Thermal monitors made from the two low-melting eutectic alloys and sealed in Pyrex tubes were included in the capsule. The composition of the two alloys and their melting points are as follows:

2.5% Ag, 97.5% Pb	Melting Point: 579°F (304°C)
1.75% Ag, 0.75% Sn, 97.5% Pb	Melting Point: 590°F (310°C)

The arrangement of the various mechanical specimens, dosimeters and thermal monitors contained in Capsule U are shown in figure 4-2.

TABLE 4-1

CHEMICAL COMPOSITION AND HEAT TREATMENT OF THE

BYRON UNIT 2 REACTOR VESSEL SURVEILLANCE MATERIALS

Element	Chemical Composition (wt%) Lower Shell Forging MK24-3		Weld Metal (a)	
C	0.18		0.09	
Mn	1.18		1.34	
P	0.005		0.01	
S	0.006		0.013	
Si	0.23		0.55	
Ni	0.65		0.65	
Mo	0.43		0.45	
Cr	0.06		0.08	
Cu	0.07		0.03	
Al	0.026		0.003	
Co	<0.01	(b)	<0.01	(b)
Pb	<0.001		<0.001	
W	<0.02		<0.02	
Ti	<0.005		<0.005	
Zr	<0.002		<0.002	
V	<0.001		<0.001	
Sn	<0.002		<0.005	
As	<0.005		0.005	
Cb	<0.003		<0.003	
N_2	0.007		0.006	
B	<0.005		0.005	

Material	Heat Treatment History Temperature (°F)	Time (Hr)	Coolant
Lower Shell (Forging MK24-3)	Austenitizing 1575-1625	9.0	Water quenched
	Tempered 1200-1250	10.25	Air cooled
	Stress Relief 1100-1200	12.75	Furnace cooled
Weld Metal(a)	Stress Relief 1100-1200	12.75	Furnace cooled

(a) This weldment was fabricated by The Babcock and Wilcox Co., using 5/32 inch weld filler wire, heat number 442002 and Linde 80 flux, lot number 8064 and is identical to that used in the actual fabrication of the reactor vessel intermediate to lower shell girth weld.

(b) Westinghouse analysis from surveillance program test plate.

TABLE 4-2

CHEMICAL COMPOSITION FOR BYRON UNIT 2 CAPSULE U IRRADIATED CHARPY IMPACT SPECIMENS

Weld Metal: Specimen No.	Chemical Composition (wt.%)[a] Cu	Ni	C	Mn	P	S	Si	Cr	Mo	V	Co
YW-6	0.024	0.740	0.080	1.401	0.008	0.013	0.496	0.085	0.397	<0.005	<0.010
YW-15	0.024	0.786	0.078	1.509	0.016	0.013	0.513	0.093	0.452	<0.005	<0.010
YW-1	0.022	0.704									
YW-2	0.020	0.681									
YW-3	0.021	0.706									
YW-4	0.020	0.697									
YW-5	0.019	0.668									
YW-7	0.022	0.759									
YW-8	0.021	0.714									
YW-9	0.020	0.678									
YW-10	0.020	0.695									
YW-11	0.019	0.689									
YW-12	0.021	0.744									
YW-13	0.022	0.738									
YW-14	0.022	0.771									
Forging MK24-3 Specimen No.	Cu	Ni	C	Mn	P	S	Si	Cr	Mo	V	Co
YT-1	0.022	0.689	0.068	1.353	0.014	0.017	0.493	0.083	0.405	<0.005	<0.010

(a) Method of analysis -- Inductively Coupled Plasma Spectrometry (ICPS) for all elements except C, S, and Si.

TABLE 4-3
CHEMISTRY RESULTS FROM THE NBS
CERTIFIED REFERENCE STANDARDS

Material ID: Low Alloy Steel: NBS Certified Reference Standards

	NBS 361		NBS 362	
	Certified	Measured (a)	Certified	Measured (a)
Metals		**Concentration in Weight Percent**		
Fe *	95.6	(matrix)	95.3	(matrix)
Mn	0.66	0.675	1.04	1.077
Cr	0.694	0.706	0.30	0.311
Ni	2.00	above calib	0.59	0.637
Mo	0.19	0.208	0.068	0.061
Co	0.032	0.033	0.30	0.354
Cu	0.042	0.045	0.50	0.529
P	0.014	0.0189	0.041	0.0472
V	0.011	0.0111	0.040	0.0398
C	0.383	0.386	0.160	0.161
S	0.014	N.A.	0.036	0.0406

Material ID: Low Alloy Steel: NBS Certified Reference Standards

	NBS 363		NBS 364	
	Certified	Measured (a)	Certified	Measured (b)
Metals		**Concentration in Weight Percent**		
Fe *	94.4	(matrix)	96.7	(matrix)
Mn	1.50	1.518	0.255	0.252
Cr	1.31	1.339	0.063	0.060
Ni	0.30	0.323	0.144	0.149
Mo	0.028	0.024	0.49	0.475
Co	0.048	0.050	0.15	0.172
Cu	0.010	0.103	0.249	0.258
P	0.029	0.0339	0.01	0.0147
V	0.31	0.276	0.105	0.105
	0.62	N.A.	0.87	N.A.
S	0.0068	N.A.	0.0250	0.0251

* Matrix element calculated as difference for material balance.
Tentative value, certified ± 100% of value.
NA - Not analyzed; NR, Not requested

(a) Method of analysis -- Inductively Coupled Plasma Spectrometry (ICPS) for all elements except C, S and Si.

TABLE 4-4

BYRON UNIT 2 REACTOR VESSEL TOUGHNESS DATA

Component	Heat No.	Material Spec. No.	Cu (%)	P (%)	Ni (%)	TNDT (°F)	50 ft/lb 35 mil Temp.(°F)	RTNDT (°F)	Upper Shelf Energy NMWD(a) (ft-lb)	Upper Shelf Energy MWD(b) (ft-lb)
Closure Head Dome	C4375-2	A533 B Cl.1	.12	.013	.65	-40	<20	-40	114	---
Closure Head Ring	48C1300-1-1	A508 Cl. 3	.05	.007	.69	-30	<30	-30	108	---
Closure Head Flange	2029-V-1	A508 Cl. 2	---	.011	.71	0	<60	0	157	---
Vessel Flange	124L556VA1	A508 Cl. 2	---	.008	.70	30	<90	30	129	---
Inlet Nozzle	51-2979	A508 Cl. 2	.07	.010	.86	-10	<50	-10	130	---
Inlet Nozzle	51-2979	A508 Cl. 2	.07	.009	.86	-20	<40	-20	121	---
Inlet Nozzle	42-5105	A508 Cl. 2	.07	.008	.84	0	<60	0	122	---
Inlet Nozzle	42-5105	A508 Cl. 2	.07	.011	.84	0	<60	0	121	---
Outlet Nozzle	11-5052	A508 Cl. 2	.09	.010	.85	-10	<50	-10	108	---
Outlet Nozzle	11-5052	A508 Cl. 2	.08	.007	.81	-10	<50	-10	121	---
Outlet Nozzle	4-2953	A508 Cl. 2	.09	.010	.78	-20	<40	-20	133	---
Outlet Nozzle	4-2956	A508 Cl. 2	.09	.009	.81	-10	<50	-10	121	---
Nozzle Shell	4P-6107	A508 Cl. 2	---	.014	.74	10	<70	10	155	---
Upper Shell	49D329/ 49C297/1-1	A508 Cl. 3	.01	.007	.70	-20	<40	-20	149	149
Lower Shell	49D330/ 49C298/1-1	A508 Cl. 3	.05	.008	.73	-20	<40	-20	127	159
Bottom Head Ring	48D1566/1-1	A508 Cl. 3	.07	.007	.67	-30	<30	-30	126	---
Bottom Head Dome	C3053-1	A533B Cl. 1	.06	.004	.64	-30	40	-20	121	---
Upper Shell to Lower Shell Girth Weld	WF447 (c)	SAW	.059	.009	.62	10	<70	10	80	---
Weld HAZ	---	---	---	---	---	-60	<0	-60	143	---

(a) Normal to major working direction.
(b) Major working direction
(c) Welded using 5/32 inch weld wire Heat No. 442002 and Linde 80 Flux Lot. No. 8064.

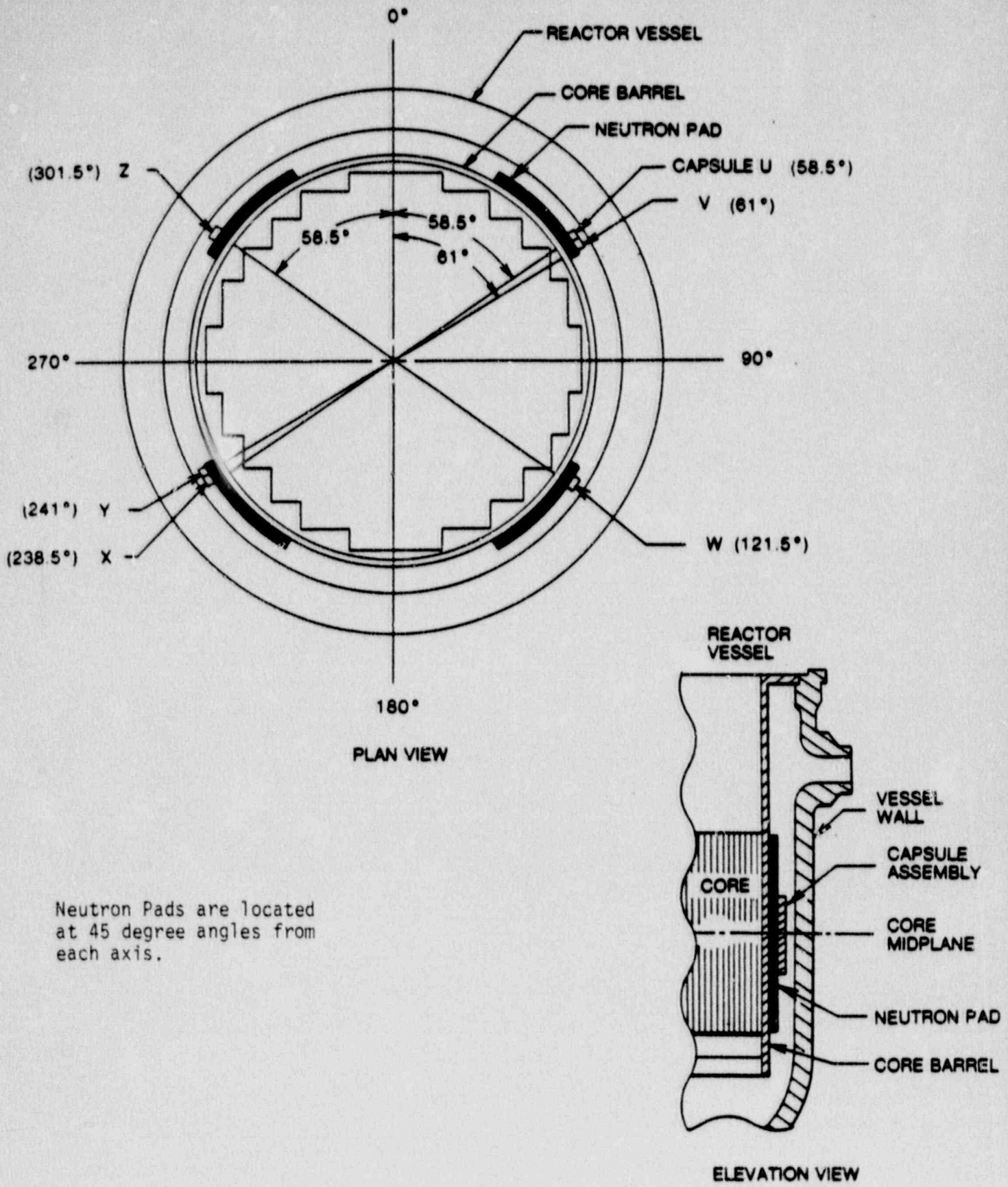

Neutron Pads are located at 45 degree angles from each axis.

Figure 4-1. Arrangement of Surveillance Capsules in the Reactor Vessel

SPECIMEN NUMBERING

LEGEND: YL - LOWER SHELL FORGING MK24-3[a] (TANGENTIAL ORIENTATION)
YT - LOWER SHELL FORGING MK24-3 (AXIAL ORIENTATION)
YW - WELD METAL
YH - HEAT-AFFECTED-ZONE MATERIAL
a. Forging Heat Number 49D330-1/49C298-1

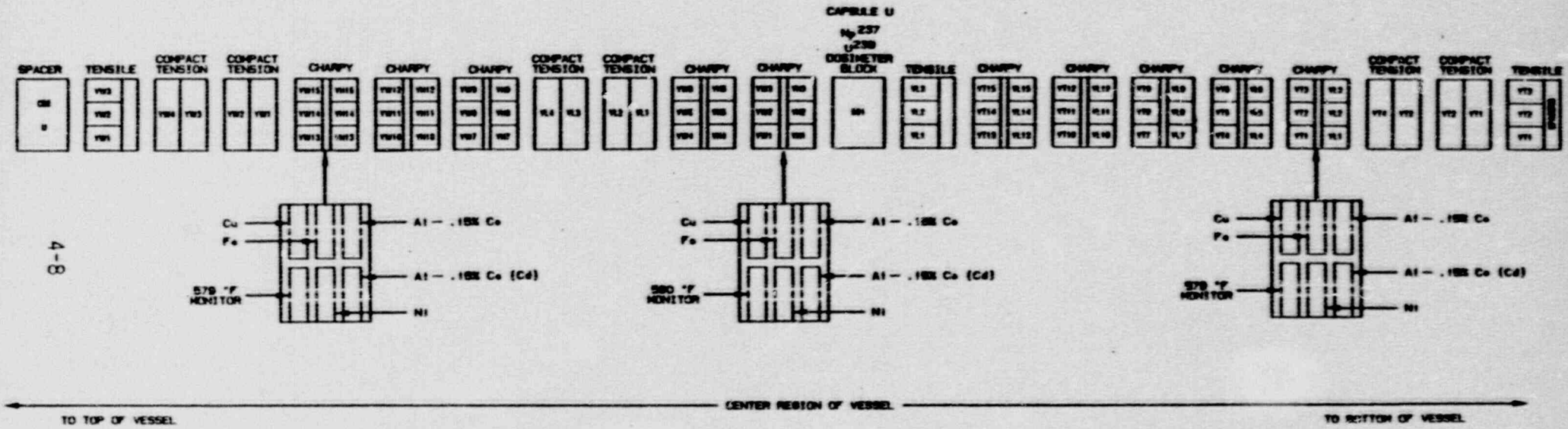

Figure 4-2. Capsule U Diagram Showing Location of Specimens, Thermal Monitors and Dosimeters

SECTION 5.0
TESTING OF SPECIMENS FROM CAPSULE U

5.1 Overview

The post-irradiation mechanical testing of the Charpy V-notch and tensile specimens was performed at the Westinghouse Science and Technology Center with consultation by Westinghouse Power Systems personnel. Testing was performed in accordance with 10CFR50, Appendices G and H,[2] ASTM Specification E185, and Westinghouse Procedure RMF-402, Revision 1 as modified by RMF Procedures 8102, Revision 1 and 8103, Revision 1.

Upon receipt of the capsule at the laboratory, the specimens and spacer blocks were carefully removed, inspected for identification number, and checked against the master list in WCAP-10395[1]. No discrepancies were found.

Examination of the two low-melting point 304°C (570°F) and 310°C (590°F) eutectic alloys indicated no melting of either type of thermal monitor. Based on this examination, the maximum temperature to which the test specimens were exposed was less than 304°C (579°F).

The Charpy impact tests were performed per ASTM Specification E23-82 and RMF Procedure 8103, Revision 1 on a Tinius-Olsen Model 74,358J machine. The tup (striker) of the Charpy machine is instrumented with an Effects Technology Model 500 instrumentation system. With this system, load-time and energy-time signals can be recorded in addition to the standard measurement of Charpy energy (E_D). From the load-time curve, the load of general yielding (P_{GY}), the time to general yielding (t_{GY}), the maximum load (P_M), and the time to maximum load (t_M) can be determined. Under some test conditions, a sharp drop in load indicative of fast fracture was observed. The load at which fast fracture was initiated is identified as the fast fracture load (P_F), and the load at which fast fracture terminated is identified as the arrest load (P_A).

The energy at maximum load (E_M) was determined by comparing the energy-time record and the load-time record. The energy at maximum load is roughly equivalent to the energy required to initiate a crack in the specimen. Therefore, the propagation energy for the crack (E_p) is the difference between the total energy to fracture (E_D) and the energy at maximum load.

The yield stress (σ_Y) is calculated from the three-point bend formula. The flow stress is calculated from the average of the yield and maximum loads, also using the three-point bend formula.

Percent shear was determined from post-fracture photographs using the ratio-of-areas methods in compliance with ASTM Specification A370-77. The lateral expansion was measured using a dial gage rig similar to that shown in the same specification.

Tension tests were performed on a 20,000-pound Instron, split-console test machine (Model 1115) per ASTM Specification E8-83 and E21-79, and RMF Procedure 8102, Revision 1. All pull rods, grips, and pins were made of Inconel 718 hardened to Rc 45. The upper pull rod was connected through a universal joint to improve axiality of loading. The tests were conducted at a constant crosshead speed of 0.05 inches per minute throughout the test.

Deflection measurements were made with a linear variable displacement transducer (LVDT) extensometer. The extensometer knife edges were spring-loaded to the specimen and operated through specimen failure. The extensometer gage length is 1.00 inch. The extensometer is rated as Class B-2 per ASTM E83-67.

Elevated test temperatures were obtained with a three-zone electric resistance split-tube furnace with a 9-inch hot zone. All tests were conducted in air.

Because of the difficulty in remotely attaching a thermocouple directly to the specimen, the following procedure was used to monitor specimen temperature. Chromel-alumel thermocouples were inserted in shallow holes in the center and each end of the gage section of a dummy specimen and in each grip. In the test configuration, with a slight load on the specimen, a plot of specimen

temperature versus upper and lower grip and controller temperatures was developed over the range of room temperature to 550°F (288°C). The upper grip was used to control the furnace temperature. During the actual testing the grip temperatures were used to obtained desired specimen temperatures. Experiments indicated that this method is accurate to ±2°F.

The yield load, ultimate load, fracture load, total elongation, and uniform elongation were determined directly from the load-extension curve. The yield strength, ultimate strength, and fracture strength were calculated using the original cross-sectional area. The final diameter and final gage length were determined from post-fracture photographs. The fracture area used to calculate the fracture stress (true stress at fracture) and percent reduction in area was computed using the final diameter measurement.

5.2 Charpy V-Notch Impact Test Results

The results of Charpy V-notch impact tests performed on the various materials contained in Capsule U irradiated to 3.96×10^{18} n/cm^2 (E > 1.0 MeV) are presented in tables 5-1 through 5-4 and are compared with unirradiated results[1] as shown in Figures 5-1 through 5-4. The transition temperature increases and upper shelf energy decreases for the Capsule U materials are summarized in Table 5-5.

Irradiation of the vessel lower shell forging MK24-3 material (tangential orientation) specimens to 3.96×10^{18} n/cm^2 (Figure 5-1) resulted in no increase in the 30 and 50 ft-lb transition temperatures and no upper shelf energy decrease. Irradiation of the vessel lower shell forging MK24-3 material (axial orientation) specimens to 3.96×10^{18} n/cm^2 (Figure 5-2) resulted in a 25°F increase in the 30 and 50 ft-lb transition temperatures and no upper shelf energy decrease.

Weld metal irradiated to 3.96×10^{18} n/cm^2 (Figure 5-3) resulted in no 30 and 50 ft-lb transition temperature increase and no upper shelf energy decrease.

Weld HAZ metal irradiated to 3.96 x 10^{18} n/cm^2 (Figure 5-4) resulted in a 30 and 50 ft-lb transition temperature increase of 25°F and no upper shelf energy decrease, respectively. A large scatter in data was observed which is typical of many HAZ Charpy tests for other surveillance programs.

The fracture appearance of each irradiated Charpy specimen from the various materials is shown in Figures 5-5 through 5-8 and show an increasingly ductile or tougher appearance with increasing test temperature.

A comparison of the 30 ft-lb transition temperature increases for the various Byron Unit 2 surveillance materials with predicted increases using the methods of NRC Regulatory Guide 1.99, Revision 2[3] is presented in Table 5-6. This comparison indicates that the transition temperature increases resulting from irradiation to 3.96 x 10^{18} n/cm^2 are less than the Guide predictions.

5.3 Tension Test Results

The results of tension tests performed on shell forging MK24-3 (tangential and axial orientation) and the weld metal irradiated to 3.96 x 10^{18} n/cm^2 are shown in Table 5-7 and are compared with unirradiated results[1] as shown in Figures 5-9, 5-10 and 5-11. Forging MK24-3 test results are shown in Figures 5-9 and 5-10 and indicated that irradiation to 3.96 x 10^{18} n/cm^2 caused a less than 5 ksi increase in the 0.2 percent offset yield strength and ultimate tensile strength. Weld metal tension tests results shown in Figure 5-11, show that the ultimate tensile strength and the 0.2 percent offset yield strength increased by less then 1 ksi with irradiation. The small increases in 0.2% yield strength and tensile strength exhibited by the forging material and weld metal indicate that these materials are not highly sensitive to radiation at 3.96 x 10^{18} n/cm^2, as is also indicated by the Charpy impact test results. The fractured tension specimens for the forging material are shown in Figures 5-12 and 5-13, while the fractured specimens for the weld metal are shown in Figure 5-14. A typical stress-strain curve for the tension tests is shown in Figure 5-15.

5.4 Compact Tension Tests

Per the surveillance capsule testing program with the Commonwealth Edison Company, 1/2 T-compact tension fracture mechanics specimens will not be tested and will be stored at the hot cells at the Westinghouse S&T Center.

TABLE 5-1

CHARPY V-NOTCH IMPACT DATA FOR THE BYRON UNIT 2 SHELL FORGING MK24-3 IRRADIATED AT 550°F, FLUENCE 3.96 x 10^{18} n/cm^2 (E > 1.0 MeV)

Sample No.	Temperature (°F)	(°C)	Impact Energy (ft-lb)	(J)	Lateral Expansion (mils)	(mm)	Shear (%)
			Axial Orientation				
YT15	-50	(-46)	9.0	(12.0)	7.0	(0.18)	5
YT4	-25	(-32)	59.0	(80.0)	45.0	(1.14)	30
YT14	-25	(-32)	14.0	(19.0)	10.0	(0.25)	10
YT1	-25	(-32)	25.0	(34.0)	20.0	(0.51)	15
YT10	-10	(-23)	32.0	(43.5)	25.0	(0.64)	25
YT9	-10	(-23)	35.0	(47.5)	29.0	(0.74)	25
YT3	0	(-18)	62.0	(84.5)	46.0	(1.17)	30
YT8	0	(-18)	62.0	(84.0)	45.0	(1.14)	30
YT13	20	(- 7)	60.0	(81.5)	48.0	(1.22)	30
YT2	50	(10)	84.0	(114.0)	56.0	(1.42)	40
YT7	72	(22)	112.0	(152.0)	68.0	(1.73)	70
YT11	150	(66)	160.0	(217.0)	85.0	(2.16)	100
YT5	250	(121)	165.0	(223.5)	78.0	(1.98)	100
YT12	350	(177)	161.0	(218.5)	79.0	(2.01)	100
YT6	400	(204)	154.0	(209.0)	79.0	(2.01)	100
			Tangential Orientation				
YL1	-80	(-62)	5.0	(7.0)	4.0	(0.10)	2
YL12	-50	(-46)	34.0	(46.0)	26.0	(0.66)	15
YL8	-50	(-46)	10.0	(13.5)	7.0	(0.18)	5
YL6	-25	(-32)	50.0	(68.0)	39.0	(0.99)	35
YL2	-25	(-32)	21.0	(28.5)	18.0	(0.46)	15
YL3	-10	(-23)	54.0	(73.0)	40.0	(1.02)	45
YL5	-10	(-23)	41.0	(55.5)	33.0	(0.84)	35
YL14	0	(-18)	68.0	(92.0)	49.0	(1.24)	55
YL10	20	(- 7)	58.0	(78.5)	42.0	(1.07)	55
YL8	50	(10)	115.0	(156.0)	79.0	(2.01)	80
YL13	72	(22)	125.0	(169.5)	81.0	(2.06)	80
YL15	150	(66)	160.0	(217.0)	89.0	(2.26)	100
YL11	250	(121)	176.0	(238.5)	88.0	(2.24)	100
YL4	350	(177)	228.0	(309.0)	74.0	(1.88)	100
YL7	400	(204)	202.0	(274.0)	73.0	(1.85)	100

TABLE 5-2

CHARPY V-NOTCH IMPACT DATA FOR THE BYRON UNIT 2 REACTOR VESSEL WELD METAL AND HAZ METAL IRRADIATED AT 550°F, FLUENCE 3.96 x 10^{18} n/cm^2 (E > 1.0 MeV)

Sample No.	Temperature (°F)	(°C)	Impact Energy (ft-lb)	(J)	Lateral Expansion (mils)	(mm)	Shear (%)
			Weld Metal				
YW12	-150	(-118)	14.0	(19.0)	9.0	(0.23)	10
YW5	-150	(-101)	18.0	(24.5)	13.0	(0.33)	15
YW2	-125	(- 87)	19.0	(26.0)	12.0	(0.30)	15
YW9	- 75	(- 59)	33.0	(44.5)	27.0	(0.69)	30
YW3	- 75	(- 59)	18.0	(24.5)	15.0	(0.38)	15
YW4	- 60	(- 51)	OPERATOR ERROR		-	-	-
YW6	- 60	(- 51)	28.0	(38.0)	22.0	(0.56)	25
YW1	- 25	(- 32)	38.0	(51.5)	32.0	(0.81)	35
YW14	- 25	(- 32)	35.0	(47.5)	30.0	(0.76)	30
YW10	25	(- 4)	56.0	(76.0)	50.0	(1.27)	55
YW7	25	(- 4)	56.0	(76.0)	48.0	(1.22)	55
YW8	72	(22)	72.0	(97.5)	60.0	(1.52)	95
YW11	150	(66)	73.0	(99.0)	64.0	(1.63)	100
YW15	260	(121)	79.0	(107.0)	69.0	(1.75)	100
YW13	350	(177)	82.0	(111.0)	71.0	(1.80)	100
			HAZ Metal				
YH13	-200	(-129)	10.0	(13.5)	5.0	(0.13)	5
YH1	-175	(-115)	59.0	(80.0)	38.0	(0.97)	40
YH3	-175	(-115)	23.0	(31.0)	10.0	(0.25)	15
YH10	-150	(-101)	32.0	(43.5)	26.0	(0.66)	25
YH6	-150	(-101)	28.0	(38.0)	15.0	(0.38)	20
YH2	-125	(- 87)	52.0	(70.5)	29.0	(0.74)	35
YH4	-125	(- 87)	109.0	(148.0)	60.0	(1.52)	70
YH12	-125	(- 87)	37.0	(50.0)	26.0	(0.66)	30
YH5	-100	(- 73)	78.0	(106.0)	46.0	(1.17)	60
YH8	-100	(- 73)	52.0	(70.5)	28.0	(0.71)	50
YH11	- 50	(- 46)	115.0	(156.0)	65.0	(1.65)	80
YH14	72	(22)	159.0	(215.5)	83.0	(2.11)	100
YH15	205	(93)	162.0	(219.5)	80.0	(2.03)	100
YH9	300	(149)	193.0	(261.5)	74.0	(1.88)	100
YH7	300	(149)	DID NOT BREAK		-	-	100

TABLE 5-3

INSTRUMENTED CHARPY IMPACT TEST RESULTS FOR THE BYRON UNIT 2

SHELL FORGING MK24-3 IRRADIATED AT 550°F, FLUENCE 3.96 x 10^{18} n/cm^2 (E > 1.0 MeV)

Sample Number	Test Temp (°F)	Charpy Energy (ft-lb)	Normalized Energies Charpy Ed/A (ft-lb/in^2)	Maximum Em/A (ft-lb/in^2)	Prop Ep/A (ft-lb/in^2)	Yield Load (kips)	Time to Yield (μsec)	Maximum Load (kips)	Time to Maximum (μsec)	Fracture Load (kips)	Arrest Load (kips)	Yield Stress (ksi)	Flow Stress (ksi)
Axial Orientation													
YT15	-50	9.0	72	34	38	2.90	95	3.90	130	2.90	0.20	95	112
YT14	-25	14.0	113	59	54	3.15	135	3.45	205	3.45	-	104	109
YT1	-25	25.0	201	157	44	3.30	85	4.10	370	4.05	-	108	122
YT4	-25	59.0	475	301	174	2.90	85	4.35	675	4.30	0.15	95	120
YT10	-10	32.0	258	203	54	2.95	80	4.10	475	4.10	0.15	98	117
YT9	-10	35.0	282	229	53	3.15	80	4.35	505	4.30	0.25	105	125
YT3	0	62.0	499	292	208	2.85	75	4.25	655	4.20	0.15	95	118
YT8	0	62.0	499	305	194	3.10	120	4.60	690	4.25	0.20	103	128
YT13	20	60.0	483	302	181	2.85	90	4.45	680	4.25	0.45	94	120
YT2	50	84.0	676	284	393	2.65	120	4.25	690	4.00	1.15	88	114
YT7	72	112.0	902	343	559	2.90	120	4.45	775	-	-	96	122
YT11	150	160.0	1288	323	965	2.65	75	4.10	765	-	-	87	111
YT5	250	165.0	1329	324	1005	2.60	70	4.00	780	-	-	86	109
YT12	350	161.0	1269	308	988	2.65	105	3.80	780	-	-	87	107
YT6	400	154.0	1240	293	947	2.05	55	3.60	755	-	-	68	93
Tangential Orientation													
YL1	-80	5.0	40	31	10	3.00	105	3.75	130	3.75	-	98	111
YL9	-50	10.0	81	32	49	2.75	125	3.80	145	3.90	-	90	108
YL12	-50	34.0	274	229	45	3.40	90	4.50	500	4.45	-	112	130
YL2	-25	21.0	169	140	30	3.40	90	4.10	335	4.10	-	113	124
YL6	-25	50.0	403	332	70	3.00	80	4.35	730	4.35	0.15	99	121
YL5	-10	41.0	330	256	74	3.00	85	4.30	580	4.30	-	101	121
YL3	-10	54.0	435	294	140	3.00	80	4.70	620	4.65	0.20	99	127
YL14	0	68.0	548	312	235	3.20	130	4.60	700	4.35	0.30	106	129
YL10	20	58.0	467	328	139	2.95	65	4.60	715	4.55	0.55	98	125
YL8	50	115.0	926	379	547	2.80	95	4.50	850	3.30	1.25	92	120
YL13	72	125.0	1007	379	627	3.10	115	4.50	850	3.05	-	107	126
YL15	150	160.0	1288	344	944	2.50	55	4.05	820	-	-	82	108
YL11	250	176.0	1417	342	1076	2.45	70	3.95	825	-	-	81	106
YL4	350	228.0	1836	265	1571	2.35	120	3.85	700	-	-	78	103
YL7	400	202.0	1629	-	-	-	-	-	-	-	-	-	-

TABLE 5-4

INSTRUMENTED CHARPY IMPACT TEST RESULTS FOR THE BYRON UNIT 2

WELD METAL AND HAZ METAL IRRADIATED AT 550°F, FLUENCE 3.96 x 10^{18} n/cm^2 (E > 1.0 MeV)

Sample Number	Test Temp (°F)	Charpy Energy (ft-lb)	Normalized Energies (ft-lb/in^2) Charpy Ed/A	Maximum Em/A	Prop Ep/A	Yield Load (kips)	Time to Yield (μsec)	Maximum Load (kips)	Time to Maximum (μsec)	Fracture Load (kips)	Arrest Load (kips)	Yield Stress (ksi)	Flow Stress (ksi)
							Weld Metal						
YW12	-180	14.0	113	80	33	3.25	90	4.45	200	4.30	-	107	127
YW5	-150	18.0	145	79	66	3.45	70	4.55	185	4.35	-	113	132
YW2	-125	19.0	153	92	61	3.45	60	4.40	205	4.30	-	113	129
YW3	- 75	18.0	145	114	31	3.50	165	3.95	345	3.95	-	116	124
YW9	- 75	33.0	266	229	37	3.25	85	4.35	495	4.35	0.15	108	126
YW4	- 60	OPERATOR ERROR	-	-	-	-	-	-	-	-	-	-	-
YW6	- 60	28.0	225	186	39	2.80	165	4.25	495	4.15	-	92	117
YW14	- 25	35.0	282	218	63	2.90	75	4.05	500	3.90	-	97	115
YW1	- 25	38.0	306	221	85	3.15	80	4.10	500	4.00	-	104	120
YW7	25	56.0	451	232	219	3.85	55	4.30	520	3.95	1.10	95	119
YW10	25	56.0	451	211	240	2.85	80	3.95	505	3.35	1.60	94	113
YW8	72	72.0	580	256	324	2.85	105	4.15	600	3.25	1.95	95	116
YW11	150	73.0	588	208	380	2.90	110	3.90	525	-	-	95	112
YW15	250	79.0	636	181	455	2.60	75	3.80	470	-	-	88	106
YW13	350	82.0	660	254	406	2.85	160	3.70	715	-	-	95	109
							HAZ Metal						
YH13	-200	10.0	81	59	21	4.00	155	4.60	210	4.55	-	132	142
YH3	-175	23.0	185	132	53	3.00	70	4.75	275	4.70	-	100	128
YH1	-175	59.0	475	368	107	3.30	105	5.05	705	4.90	0.20	109	138
YH6	-150	28.0	225	187	39	3.25	50	4.85	360	4.85	-	107	134
YH10	-150	32.0	258	191	66	3.50	70	4.90	385	4.85	-	115	138
YH12	-125	37.0	298	92	206	1.95	85	3.70	275	-	-	64	93
YH2	-125	52.0	419	360	58	3.20	120	5.25	695	4.95	-	105	140
YH4	-125	109.0	878	337	541	3.60	115	4.90	690	3.70	0.35	119	141
YH8	-100	52.0	419	340	79	3.05	125	3.90	705	4.90	0.35	101	131
YH5	-100	78.0	628	339	289	3.75	90	4.90	665	4.55	-	124	143
YH11	- 50	115.0	926	378	548	3.40	90	4.80	765	3.65	1.10	113	135
YH14	72	159.0	1280	329	952	3.15	105	4.70	690	-	-	105	130
YH15	200	162.0	1304	268	1036	2.00	45	3.40	775	-	-	66	89
YH9	300	193.0	1554	278	1276	2.20	85	3.25	825	-	-	72	90
YH7	300	DID NOT BREAK	-	-	-	-	-	-					

TABLE 5-5

EFFECT OF 550°F IRRADIATION AT 3.96×10^{18} n/cm^2 (E > 1.0 MeV)

ON NOTCH TOUGHNESS PROPERTIES OF BYRON UNIT 2 REACTOR VESSEL MATERIALS

Material	Average 30 ft-lb Temperature (°F)			Average 35 mil Lateral Expansion Temperature (°F)			Average 50 ft-lb Temperature (°F)			Average Energy Absorption at Full Shear (ft-lb)		
	Unirradiated	Irradiated	ΔT	Unirradiated	Irradiated	ΔT	Unirradiated	Irradiated	ΔT	Unirradiated	Irradiated	Δ(ft-lb)
Forging MK24-3 (Tangential)	-30	-30	0	-25	-25	0	-25	-25	0	170	170	0
Forging MK24-3 (Axial)	-50	-25	25	-35	-10	25	-30	-5	25	154	154	0
Weld Metal	-65	-65	0	-25	-25	0	0	0	0	67	67	0
HAZ Metal	-170	-145	25	-135	-110	25	-150	-125	25	131	131	0

TABLE 5-6

COMPARISON OF BYRON UNIT 2 30 FT-LB TRANSITION TEMPERATURE SHIFTS

AND UPPER SHELF ENERGY DECREASES WITH REGULATORY GUIDE 1.99 REVISION 2 PREDICTIONS

		30 ft-lb Transition Temp. Shift		Upper Shelf Energy Decrease	
	Fluence	R.G. 1.99 Rev. 2 (Predicted)	Capsule U	R.G. 1.99 Rev. 2	Capsule U
Material	10^{18} n/cm^2	(°F)	(°F)	(°F)	(°F)
Forging MK24-3 (Tang.)	3.96	15.0	0	15	0
Forging MK24-3 (Axial)	3.96	15.0	0	15	0
Weld Metal	3.96	30.0	0	15	0

a) Cu and Ni values from table 4-1 were used to determine R.G. 1.99 predictions.

TABLE 5-7

TENSILE PROPERTIES FOR BYRON UNIT 2 REACTOR VESSEL MATERIAL

IRRADIATED AT 550°F TO 3.96 x 10^{18} n/cm^2 (E > 1.0 MeV)

Material	Sample Number	Test Temp. (°F)	0.2% Yield Strength (ksi)	Ultimate Strength (ksi)	Fracture Load (kip)	Fracture Stress (ksi)	Fracture Strength (ksi)	Uniform Elongation (%)	Total Elongation (%)	Reduction in Area (%)
Forging MK24-3 (Axial Orient.)	YT1	78	67.7	88.6	2.75	163.8	56.0	13.5	28.1	69
	YT2	300	60.8	79.5	2.15	154.1	43.8	10.5	23.2	69
	YT3	550	59.1	85.6	2.70	209.2	55.0	10.5	22.4	63
Forging MK24-3 (Tangential Orient.)	YL1	78	68.8	89.6	2.55	182.7	51.9	14.2	30.6	72
	YL2	300	61.6	80.5	2.50	172.4	50.9	11.3	24.9	70
	YL3	550	59.1	85.6	2.65	142.6	54.0	10.5	30.5	62
Weld Metal	YW1	78	71.3	88.6	3.15	144.3	64.2	10.5	21.0	56
	YW2	300	63.7	79.5	2.95	148.8	60.1	9.8	18.9	60
	YW3	550	63.7	80.5	3.00	192.1	61.1	9.0	18.0	68

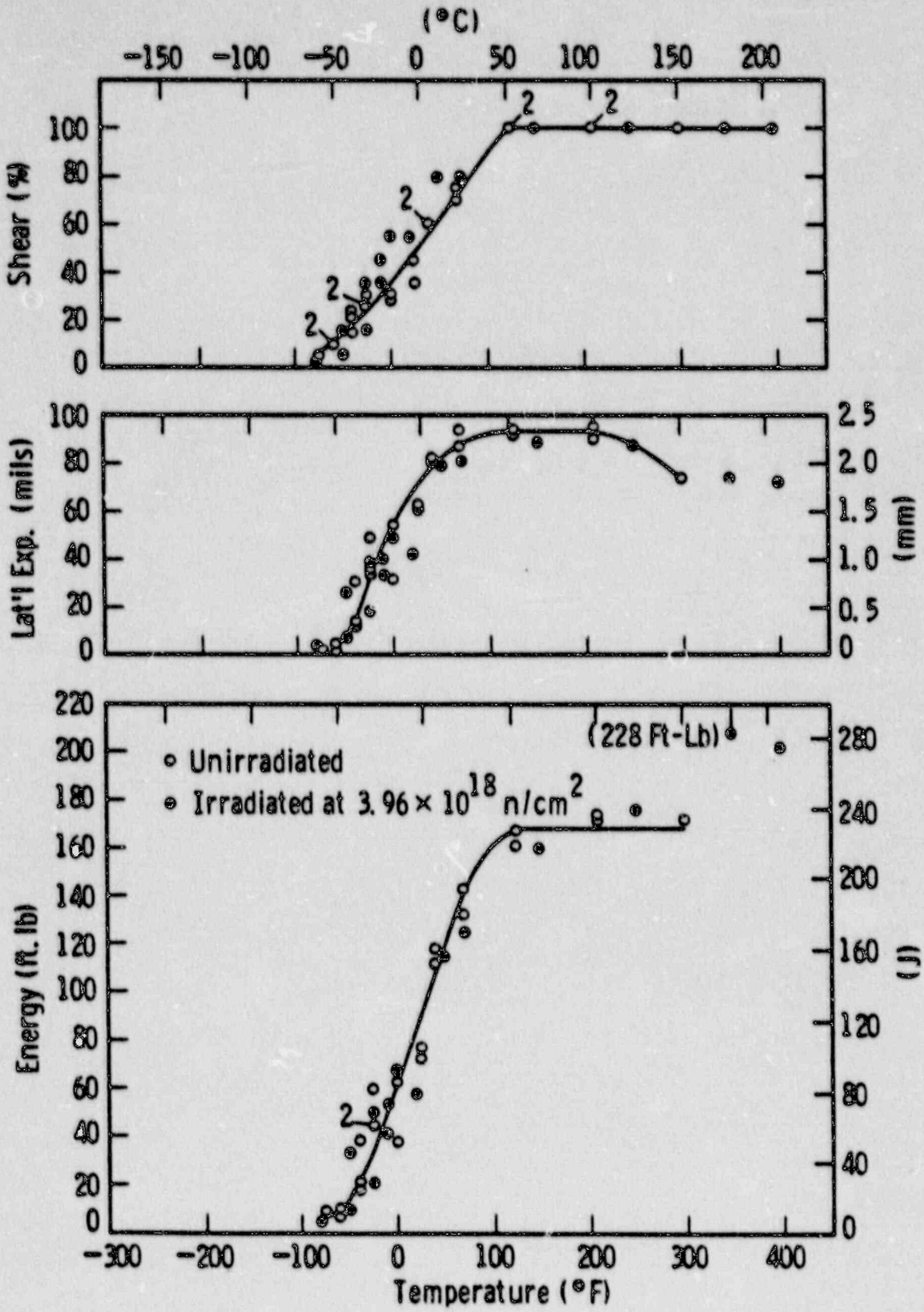

Figure 5-1. Charpy V-Notch Impact Properties for Byron Unit 2 Reactor Vessel Shell Forging MK24-3 (Tangential Orientation)

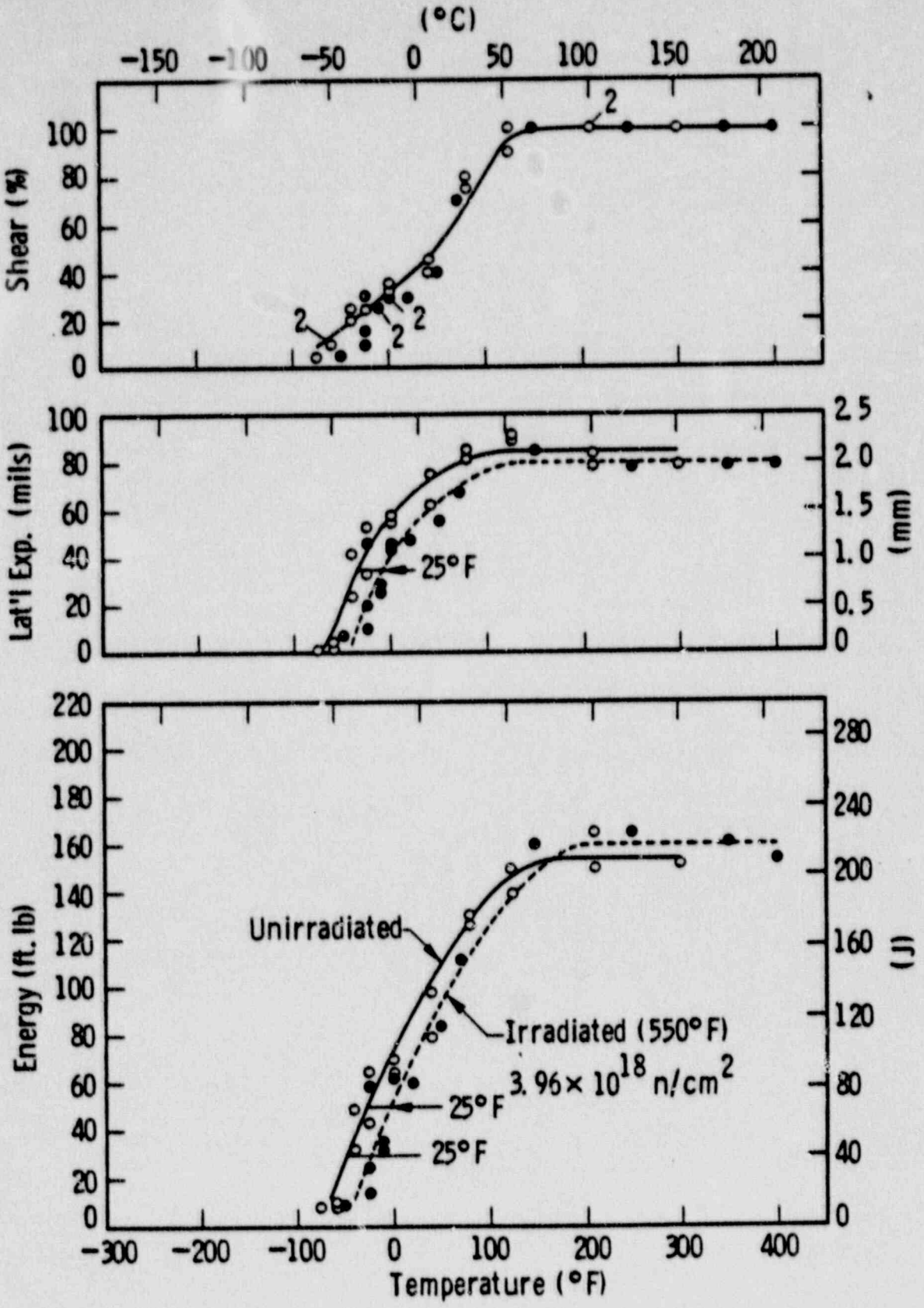

Figure 5-2. Charpy V-Notch Impact Properties for Byron Unit 2 Reactor Vessel Shell Forging MK24-3 (Axial Orientation)

Curve 757608-A

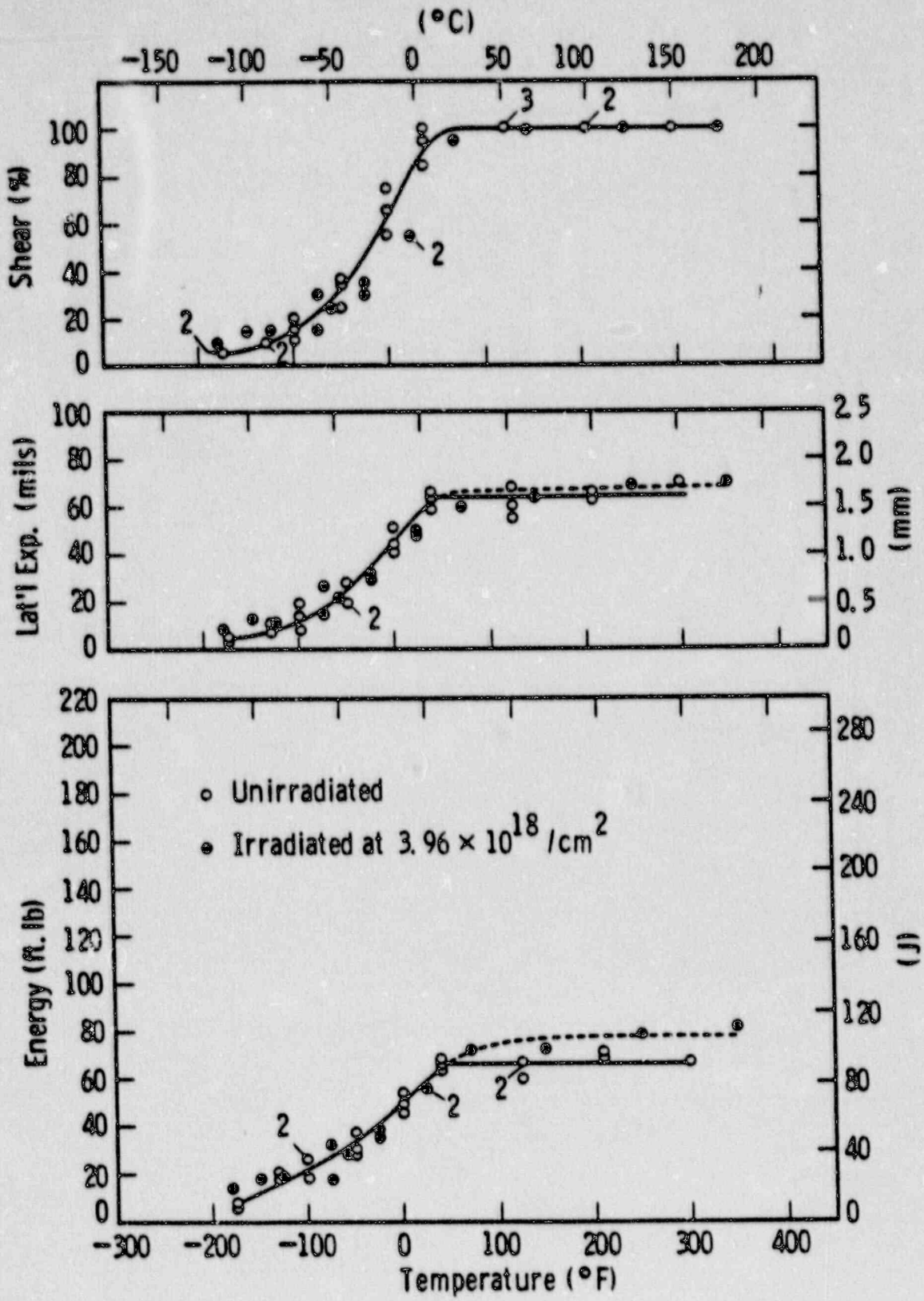

Figure 5-3. Charpy V-Notch Impact Properties for Byron Unit 2 Reactor Vessel Weld Metal

Curve 757610-A

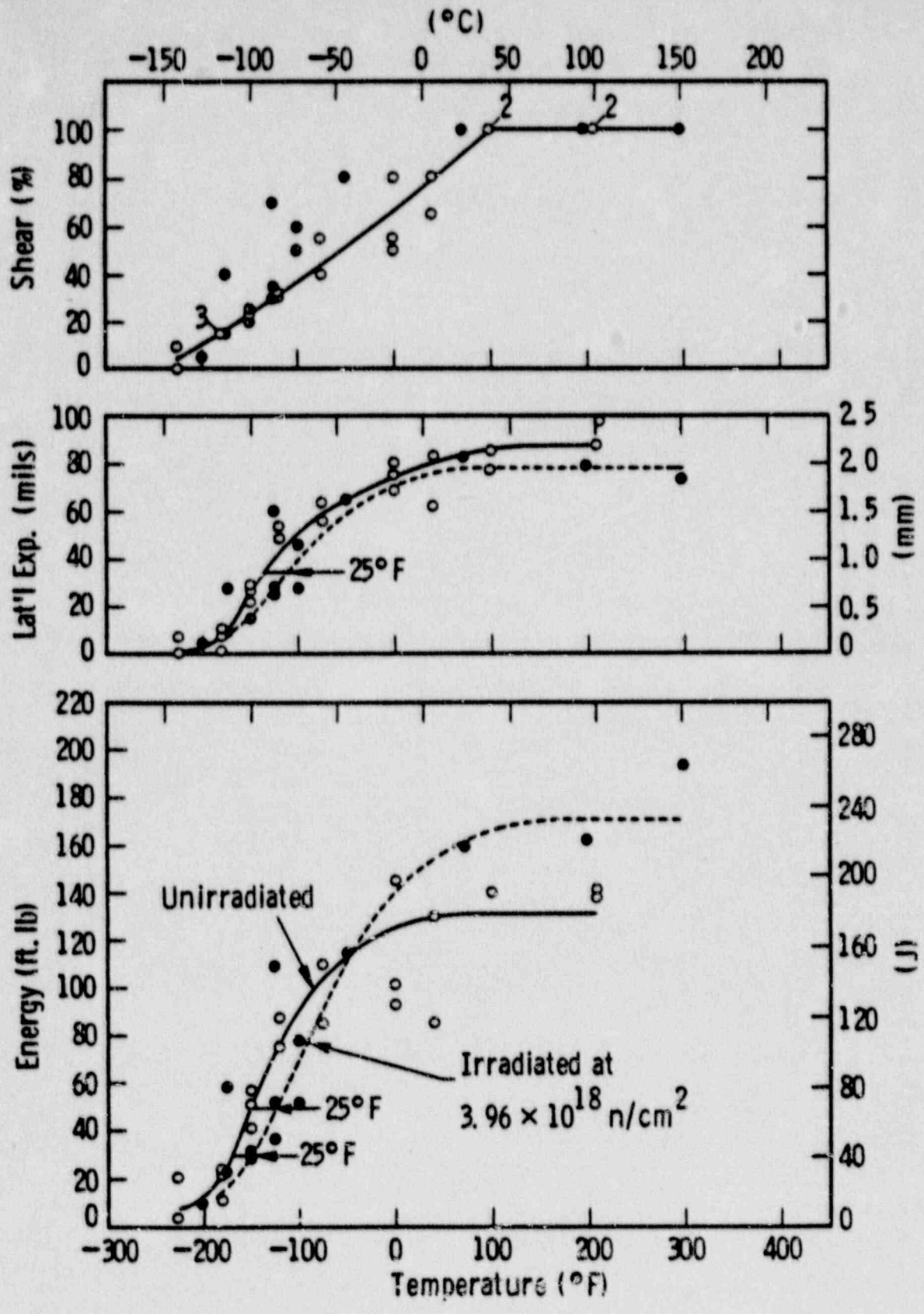

Figure 5-4. Charpy V-Notch Impact Properties for Byron Unit 2 Reactor Weld Heat Affected Zone Metal

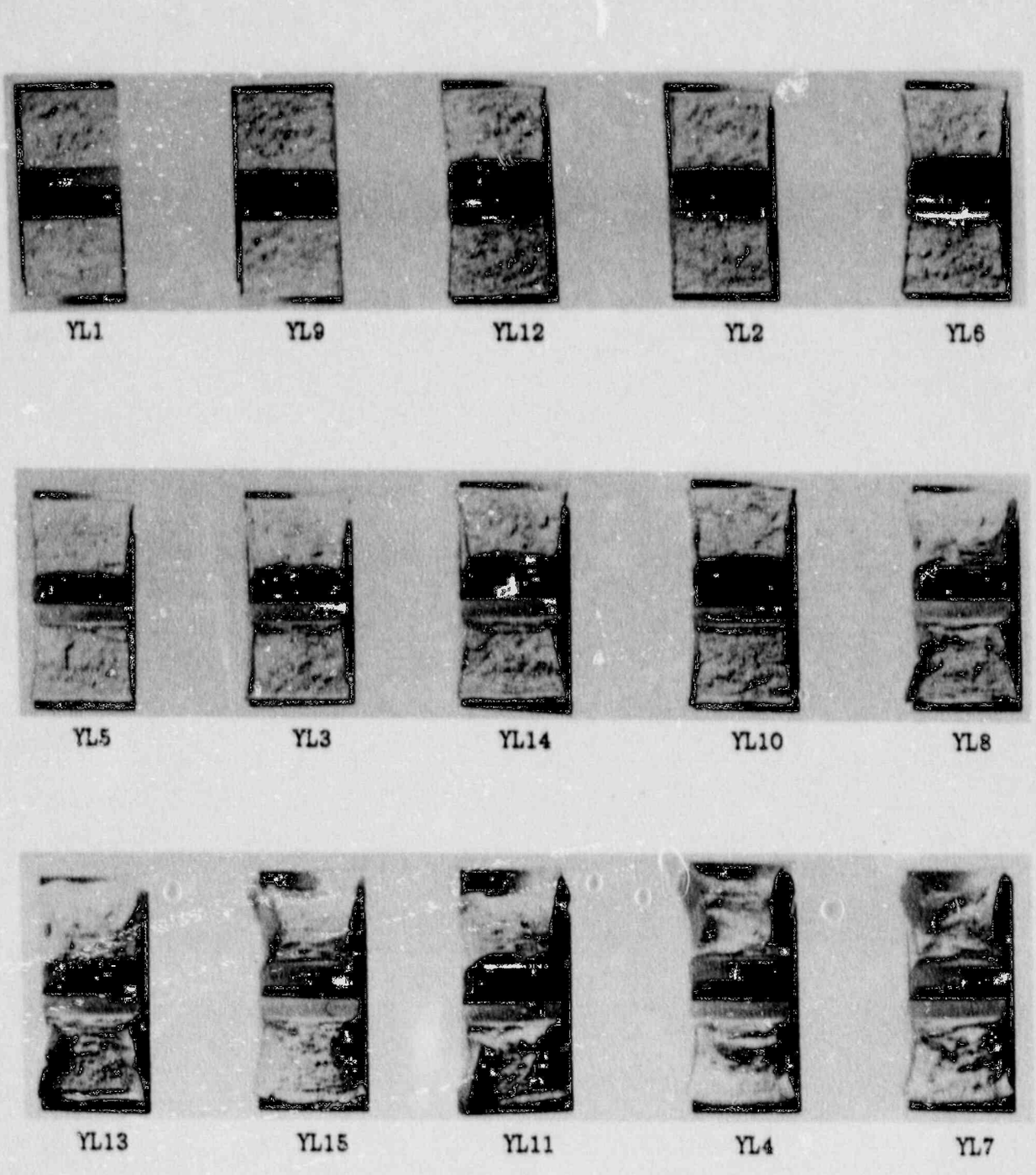

Figure 5-5. Charpy Impact Specimen Fracture Surfaces for Byron Unit 2 Reactor Vessel Shell Forging MK24-3 (Tangential Orientation)

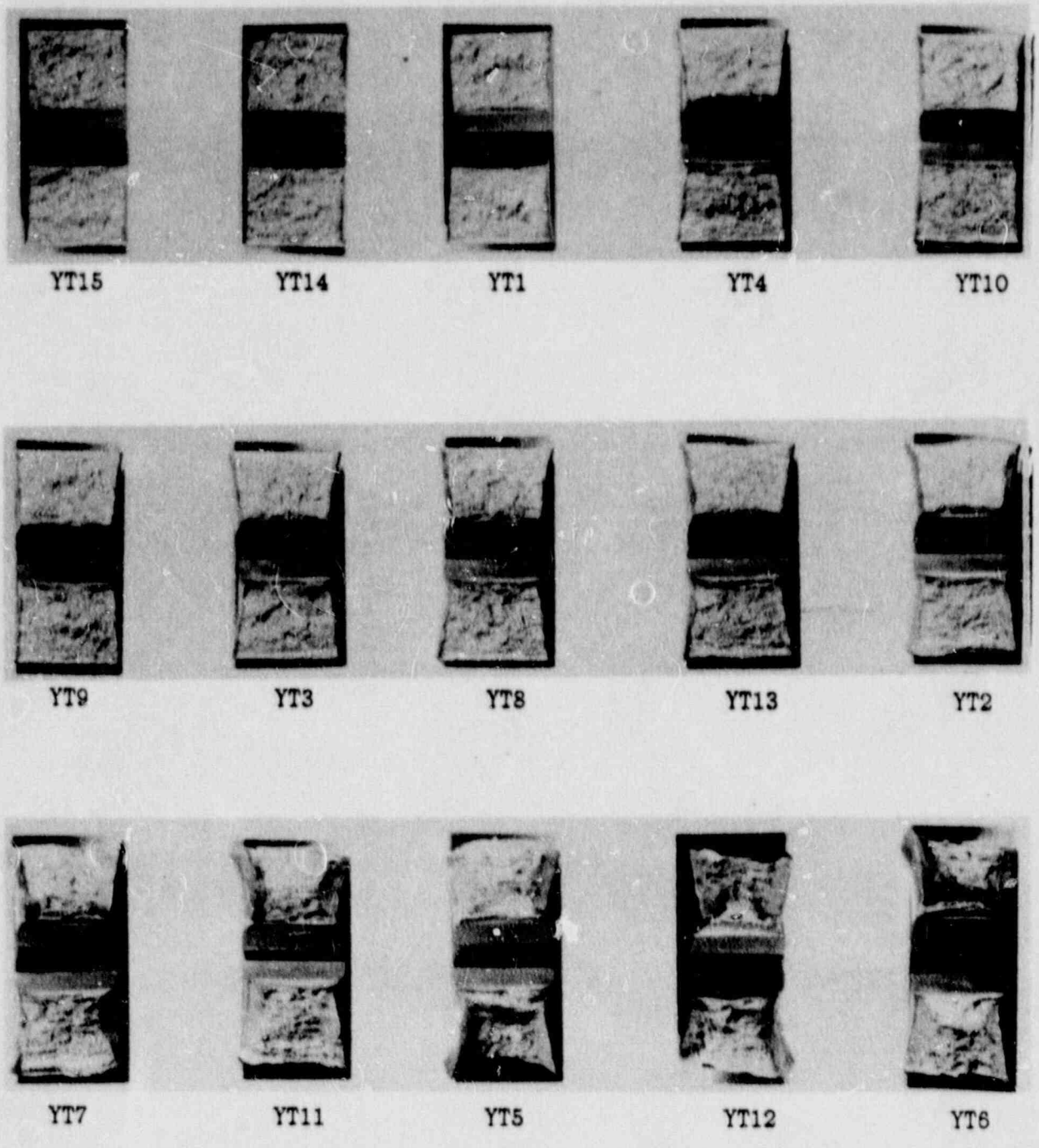

Figure 5-6. Charpy Impact Specimen Fracture Surfaces for Byron Unit 2 Reactor Vessel Shell Forging MK24-3 (Axial Orientation)

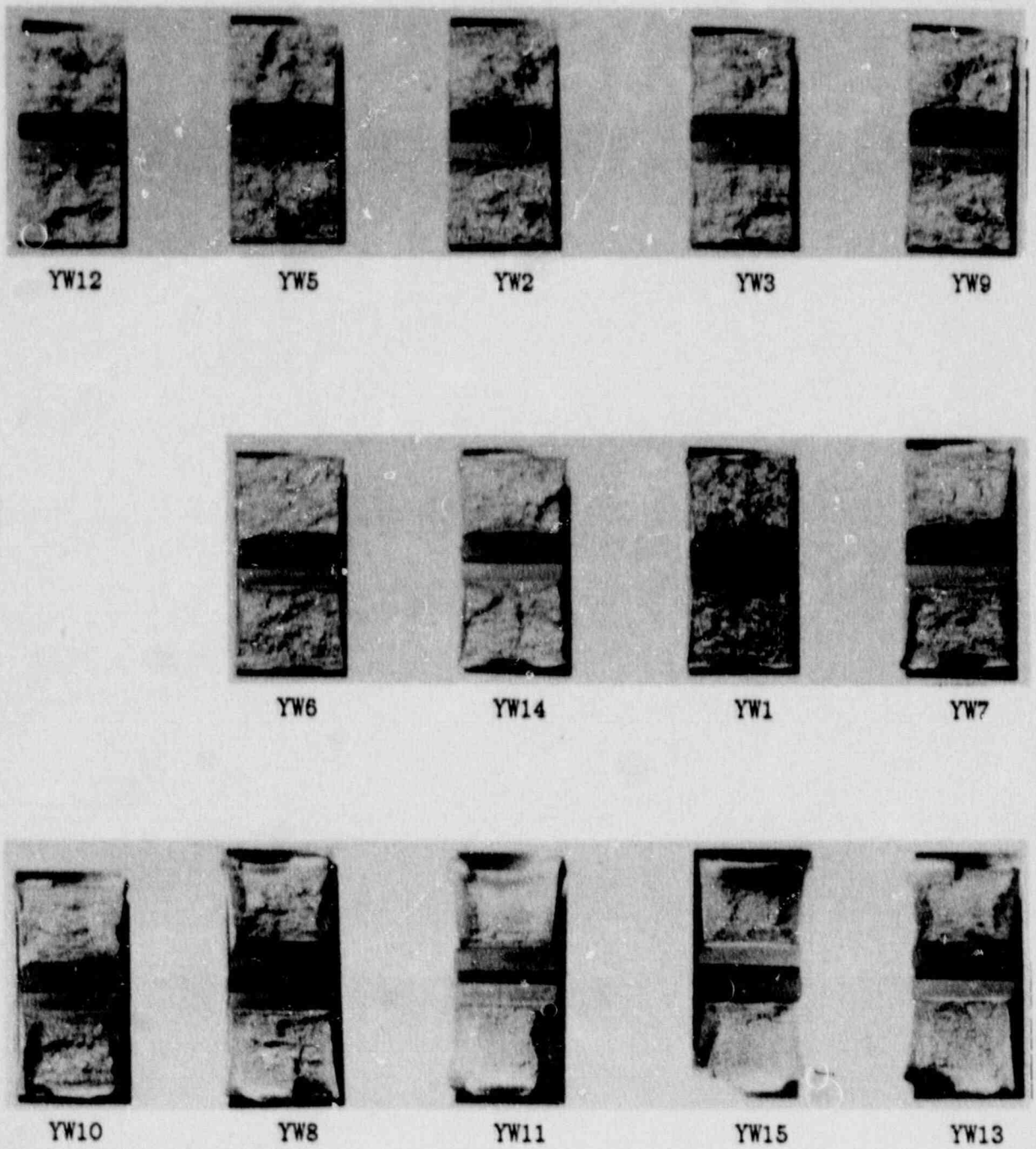

Figure 5-7. Charpy Impact Specimen Fracture Surfaces for Byron Unit 2 Reactor Vessel Weld Metal

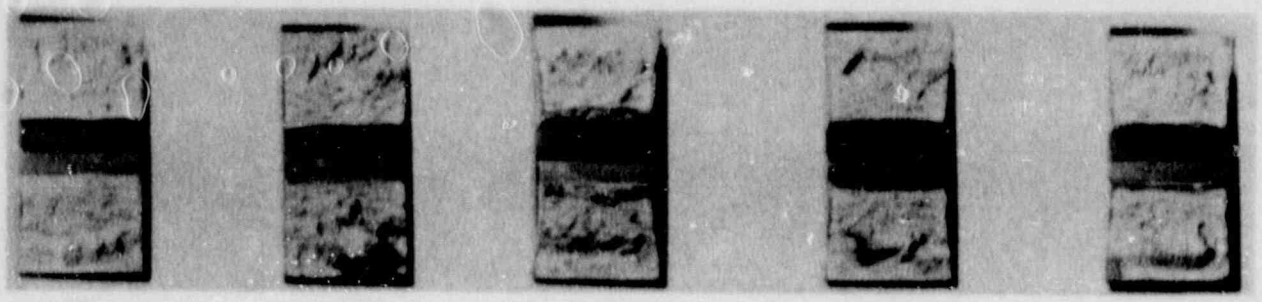

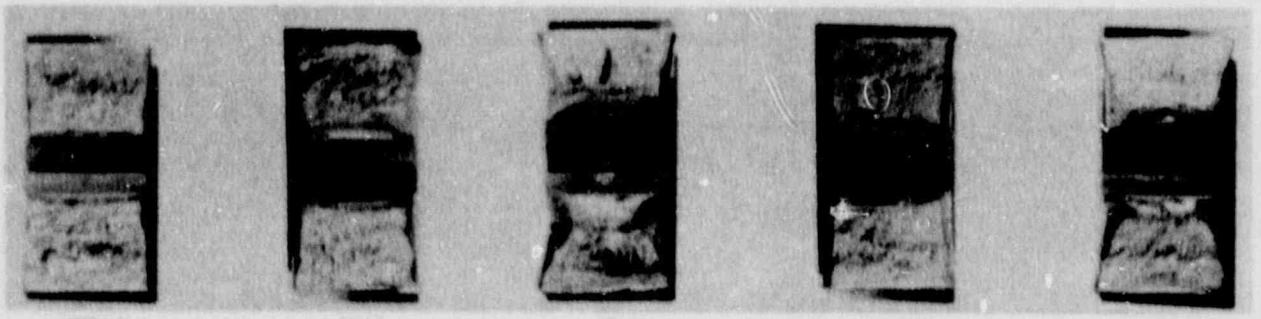

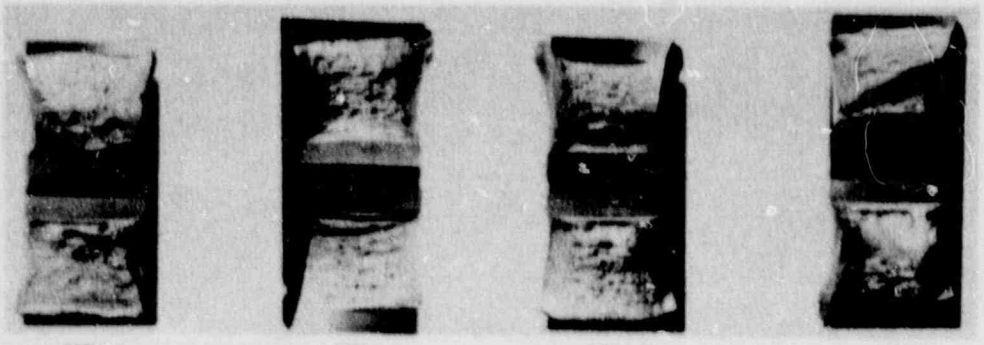

Figure 5-8. Charpy Impact Specimen Fracture Surfaces for Byron Unit 2 Reactor Vessel Weld Heat Affected Zone (HAZ) Metal

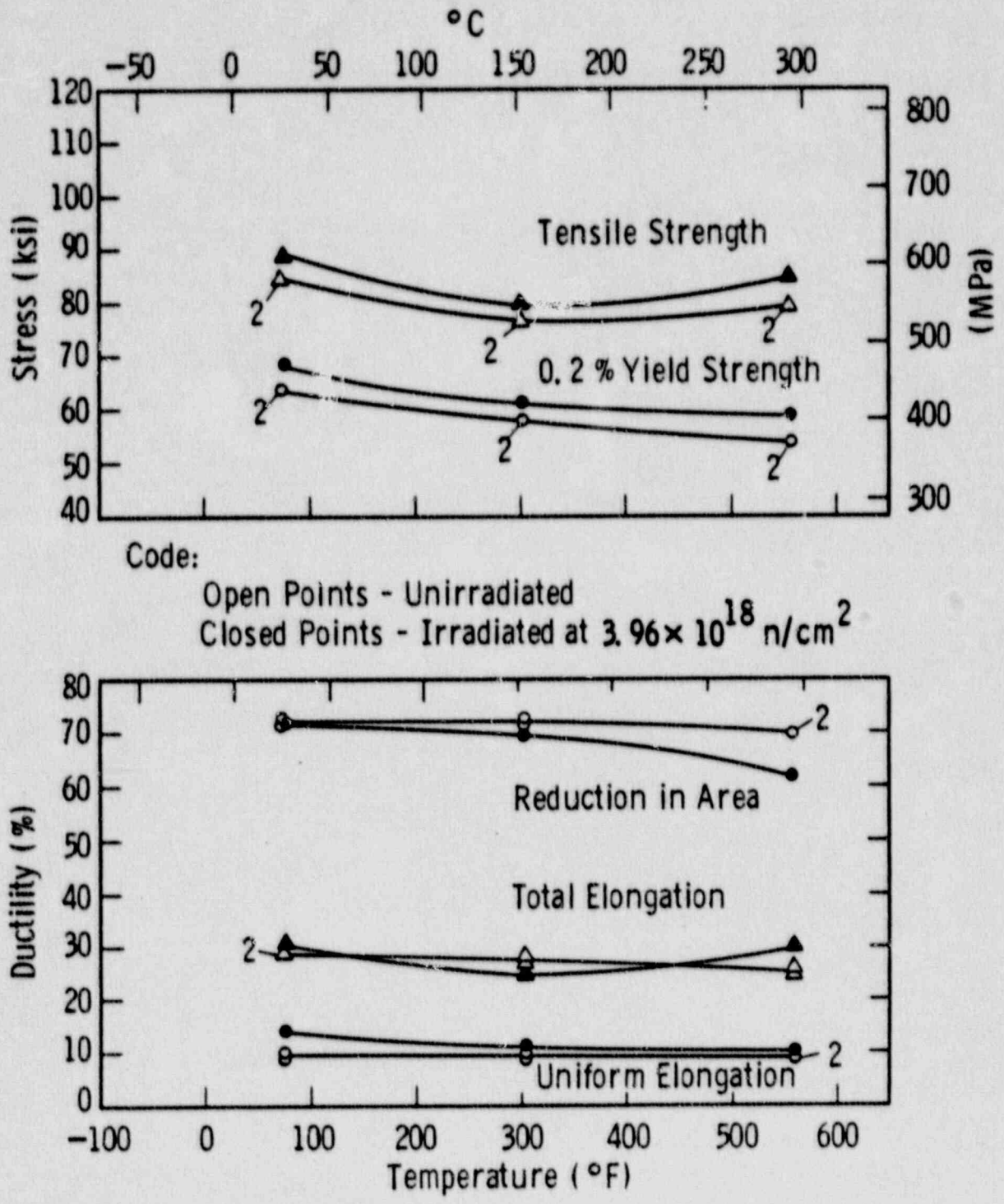

Figure 5-9. Tensile Properties for Byron Unit 2 Reactor Vessel Shell Forging MK24-3 (Tangential Orientation)

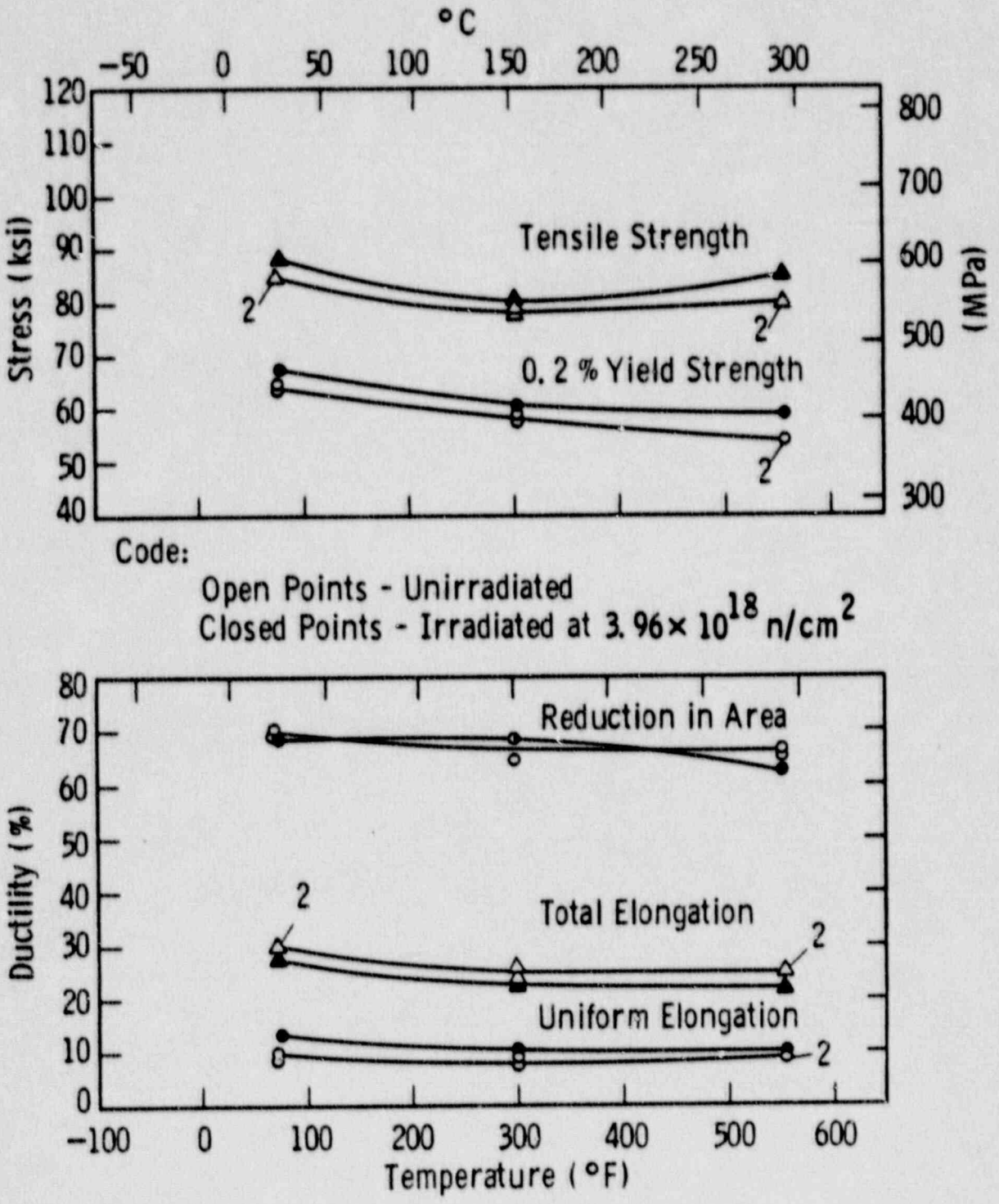

Figure 5-10. Tensile Properties for Byron Unit 2 Reactor Vessel Shell Forging MK24-3 (Axial Orientation)

Curve 757614-A

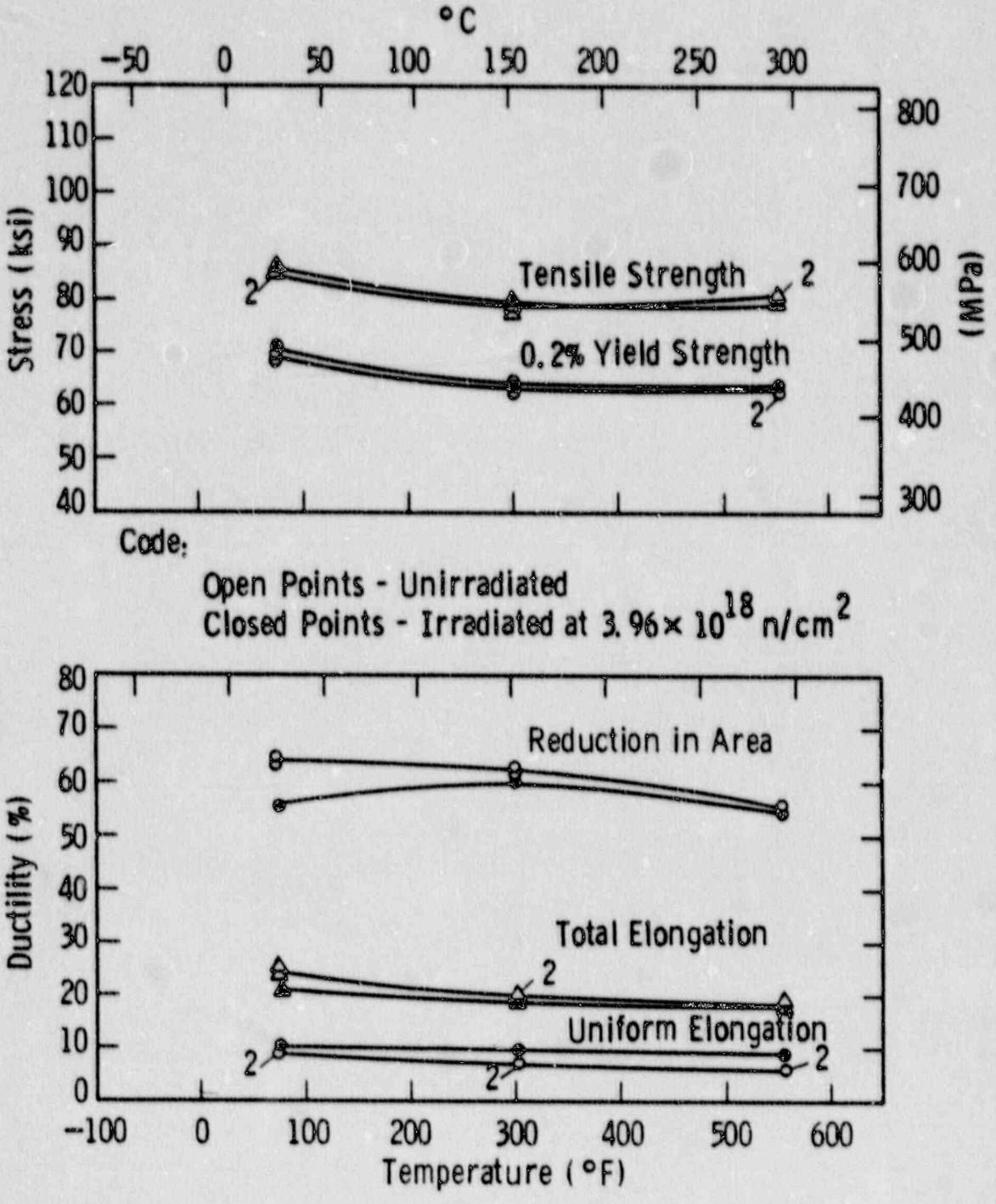

Figure 5-11. Tensile Properties for Byron Unit 2 Reactor Vessel Weld Metal

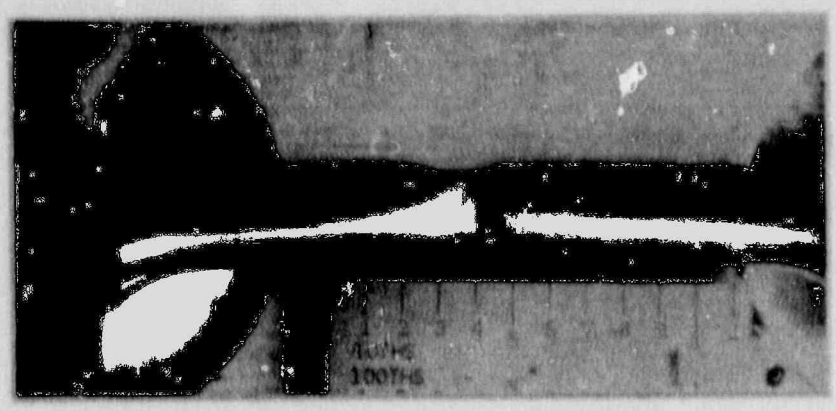

Specimen YL1 78°F

Specimen YL2 300°F

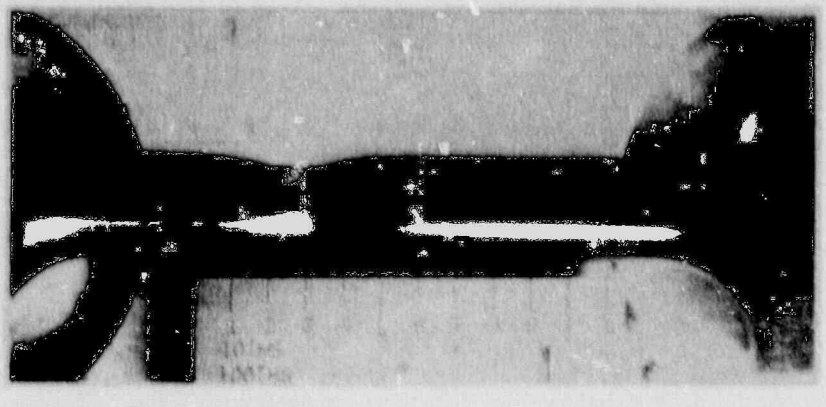

Specimen YL3 550°F

Figure 5-12. Fractured Tensile Specimens from Byron Unit 2 Reactor Vessel Shell Forging MK24-3 (Tangential Orientation)

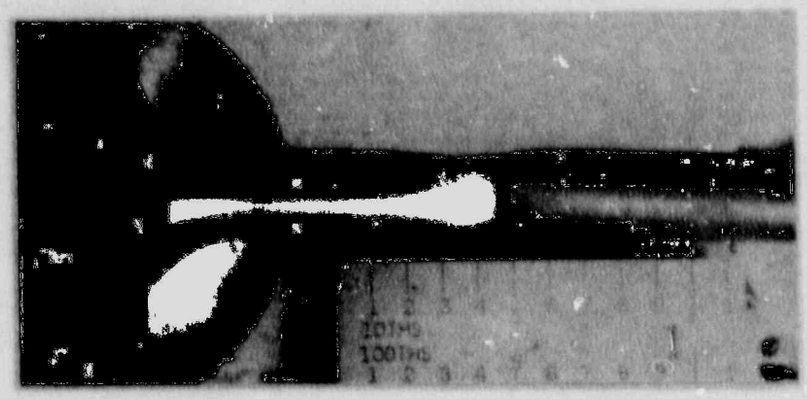

Specimen YT1 78°F

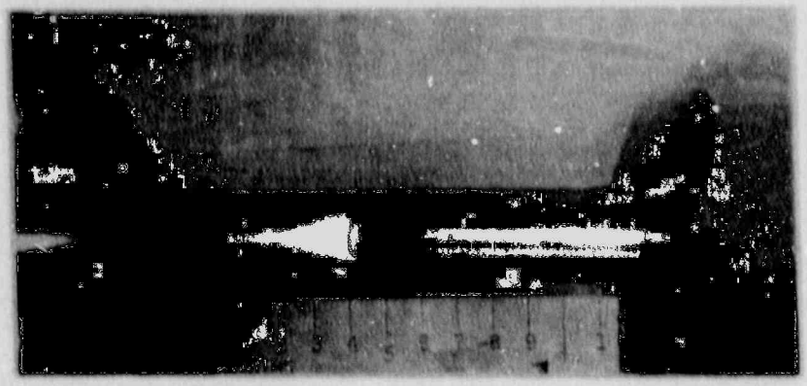

Specimen YT2 300°F

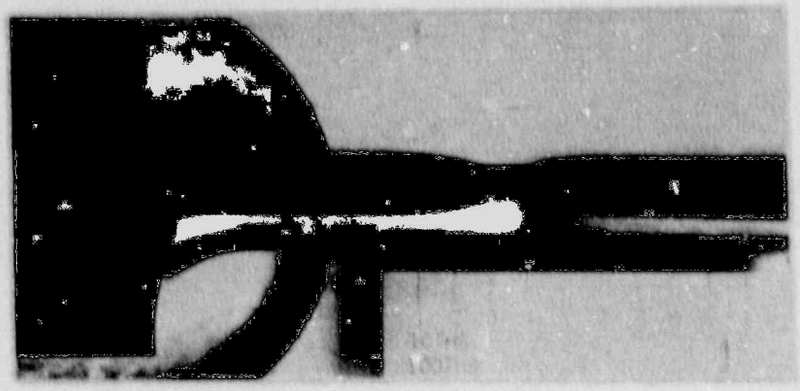

Specimen YT3 550°F

Figure 5-13. Fractured Tensile Specimens from Byron Unit 2 Reactor Vessel Shell Forging MK24-3 (Axial Orientation)

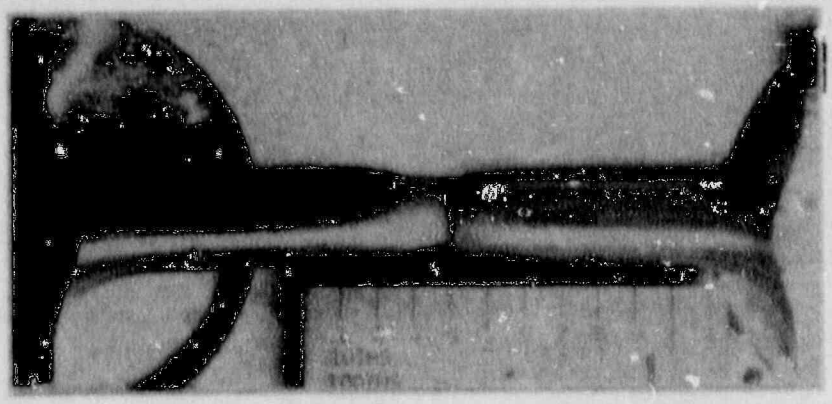

Specimen YW1 78°F

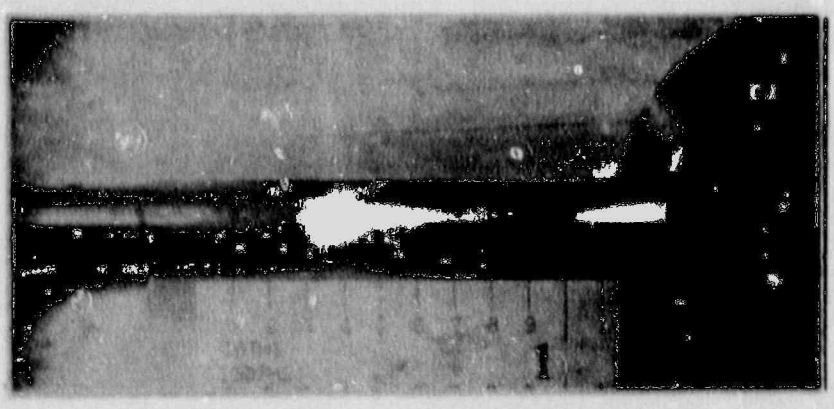

Specimen YW2 300°F

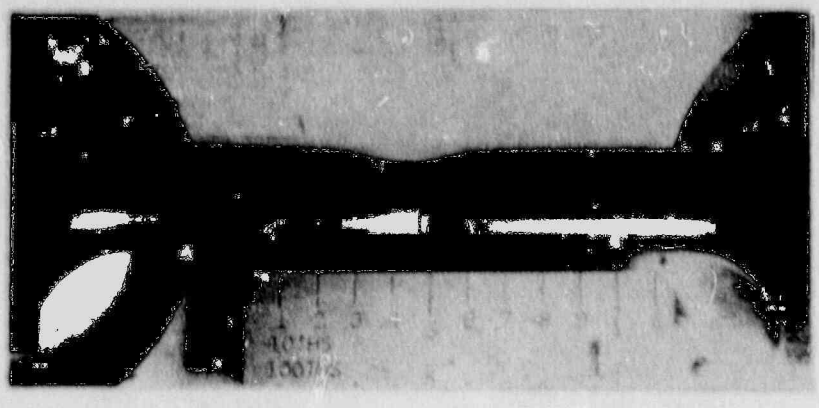

Specimen YW3 550°F

Figure 5-14. Fractured Tensile Specimens from Byron Unit 2 Reactor Vessel Weld Metal

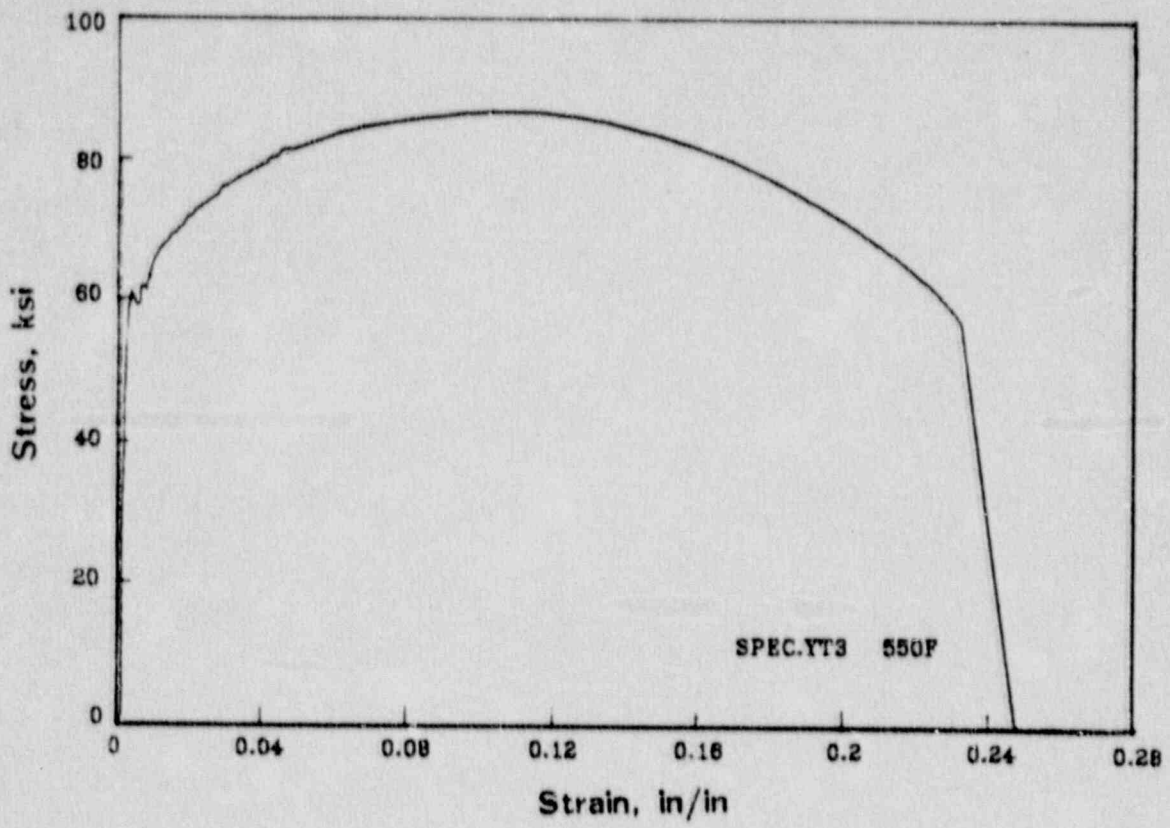

Figure 5-15. Typical Stress-Strain Curve for Commonwealth Edison Company Byron Station Unit 2 Shell Forging MK24-3 Tension Specimens.

SECTION 6.0
RADIATION ANALYSIS AND NEUTRON DOSIMETRY

6.1 Introduction

Knowledge of the neutron environment within the reactor pressure vessel and surveillance capsule geometry is required as an integral part of LWR reactor pressure vessel surveillance programs for two reasons. First, in order to interpret the neutron radiation-induced material property changes observed in the test specimens, the neutron environment (energy spectrum, flux, fluence) to which the test specimens were exposed must be known. Second, in order to relate the changes observed in the test specimens to the present and future condition of the reactor vessel, a relationship must be established between the neutron environment at various positions within the reactor vessel and that experienced by the test specimens. The former requirement is normally met by employing a combination of rigorous analytical techniques and measurements obtained with passive neutron flux monitors contained in each of the surveillance capsules. The latter information is derived solely from analysis.

The use of fast neutron fluence ($E > 1.0$ MeV) to correlate measured materials properties changes to the neutron exposure of the material for light water reactor applications has traditionally been accepted for development of damage trend curves as well as for the implementation of trend curve data to assess vessel condition. In recent years, however, it has been suggested that an exposure model that accounts for differences in neutron energy spectra between surveillance capsule locations and positions within the vessel wall could lead to an improvement in the uncertainties associated with damage trend curves as well as to a more accurate evaluation of damage gradients through the pressure vessel wall.

Because of this potential shift away from a threshold fluence toward an energy dependent damage function for data correlation, ASTM Standard Practice E853, "Analysis and Interpretation of Light Water Reactor Surveillance Results," recommends reporting displacements per iron atom (dpa) along with fluence

(E > 1.0 MeV) to provide a data base for future reference. The energy dependent dpa function to be used for this evaluation is specified in ASTM Standard Practice E693, "Characterizing Neutron Exposures in Ferritic Steels in Terms of Displacements per Atom." The application of the dpa parameter to the assessment of embrittlement gradients through the thickness of the pressure vessel wall has already been promulgated in Revision 2 to the Regulatory Guide 1.99, "Radiation Damage to Reactor Vessel Materials."

This section provides the results of the neutron dosimetry evaluations performed in conjunction with the analysis of test specimens contained in surveillance capsule U. Fast neutron exposure parameters in terms of fast neutron fluence (E > 1.0 MeV), fast neutron fluence (E > 0.1 Mev), and iron atom displacements (dpa) are established for the capsule irradiation history. The analytical formalism relating the measured capsule exposure to the exposure of the vessel wall is described and used to project the integrated exposure of the vessel itself. Also uncertainties associated with the derived exposure parameters at the surveillance capsule and with the projected exposure of the pressure vessel are provided.

6.2 Discrete Ordinates Analysis

A plan view of the reactor geometry at the core midplane is shown in Figure 4-1. Six irradiation capsules attached to the neutron pads are included in the reactor design to constitute the reactor vessel surveillance program. The capsules are located at azimuthal angles of 58.5°, 61.0°, 121.5°, 238.5°, 241.0°, and 301.5° relative to the core cardinal axes as shown in Figure 4-1.

A plan view of a dual surveillance capsule holder attached to the neutron pad is shown in Figure 6-1. The stainless steel specimen containers are 1.182 by 1-inch and approximately 56 inches in height. The containers are positioned axially such that the specimens are centered on the core midplane, thus spanning the central 5 feet of the 12-foot high reactor core.

From a neutron transport standpoint, the surveillance capsule structures are significant. They have a marked effect on both the distribution of neutron flux and the neutron energy spectrum in the water annulus between the neutron pad and the reactor vessel. In order to properly determine the neutron environment at the test specimen locations, the capsules themselves must be included in the analytical model.

In performing the fast neutron exposure evaluations for the surveillance capsules and reactor vessel, two distinct sets of transport calculations were carried out. The first, a single computation in the conventional forward mode, was used primarily to obtain relative neutron energy distributions throughout the reactor geometry as well as to establish relative radial distributions of exposure parameters ($\phi(E > 1.0$ Mev), $\phi(E > 0.1$ Mev), and dpa) through the vessel wall. The neutron spectral information was required for the interpretation of neutron dosimetry withdrawn from the surveillance capsule as well as for the determination of exposure parameter ratios; i.e., dpa/$\phi(E > 1.0$ MeV), within the pressure vessel geometry. The relative radial gradient information was required to permit the projection of measured exposure parameters to locations interior to the pressure vessel wall; i.e., the 1/4T, 1/2T, and 3/4T locations.

The second set of calculations consisted of a series of adjoint analyses relating the fast neutron flux ($E > 1.0$ MeV) at surveillance capsule positions, and several azimuthal locations on the pressure vessel inner radius to neutron source distributions within the reactor core. The importance functions generated from these adjoint analyses provided the basis for all absolute exposure projections and comparison with measurement. These importance functions, when combined with cycle specific neutron source distributions, yielded absolute predictions of neutron exposure at the locations of interest for the cycle 1 irradiation; and established the means to perform similar predictions and dosimetry evaluations for all subsequent fuel cycles. It is important to note that the cycle specific neutron source distributions utilized in these analyses included not only spatial variations of fission rates within the reactor core; but, also accounted for the effects

of varying neutron yield per fission and fission spectrum introduced by the build-up of plutonium as the burnup of individual fuel assemblies increased.

The absolute cycle specific data from the adjoint evaluations together with relative neutron energy spectra and radial distribution information from the forward calculation provided the means to:

1. Evaluate neutron dosimetry obtained from surveillance capsule locations.

2. Extrapolate dosimetry results to key locations at the inner radius and through the thickness of the pressure vessel wall.

3. Enable a direct comparison of analytical prediction with measurement.

4. Establish a mechanism for projection of pressure vessel exposure as the design of each new fuel cycle evolves.

The forward transport calculation for the reactor model summarized in Figures 4-1 and 6-1 was carried out in R, θ geometry using the DOT two-dimensional discrete ordinates code [4] and the SAILOR cross-section library [5]. The SAILOR library is a 47 group ENDFB-IV based data set produced specifically for light water reactor applications. In these analyses anisotopic scattering was treated with a P_3 expansion of the cross-sections and the angular discretization was modeled with an S_8 order of angular quadrature.

The reference core power distribution utilized in the forward analysis was derived from statistical studies of long-term operation of Westinghouse 4-loop plants. Inherent in the development of this reference core power distribution is the use of an out-in fuel management strategy; i.e., fresh fuel on the core periphery. Furthermore, for the peripheral fuel assemblies, a 2σ uncertainty derived from the statistical evaluation of plant to plant and cycle to cycle variations in peripheral power was used. Since it is unlikely that a single reactor would have a power distribution at the nominal +2σ

level for a large number of fuel cycles, the use of this reference distribution is expected to yield somewhat conservative results.

All adjoint analyses were also carried out using an S_8 order of angular quadrature and the P_3 cross-section approximation from the SAILOR library. Adjoint source locations were chosen at several azimuthal locations along the pressure vessel inner radius as well as the geometric center of each surveillance capsule. Again, these calculations were run in R, θ geometry to provide neutron source distribution importance functions for the exposure parameter of interest; in this case, ϕ (E > 1.0 MeV). Having the importance functions and appropriate core source distributions, the response of interest could be calculated as:

$$R(r, \theta) = \int_r \int_\theta \int_E I(r, \theta, E)\, S(r, \theta, E)\, r\, dr\, d\theta\, dE$$

where: $R(r, \theta)$ = ϕ (E > 1.0 MeV) at radius r and azimuthal angle θ

$I(r, \theta, E)$ = Adjoint importance function at radius, r, azimuthal angle θ, and neutron source energy E.

$S(r, \theta, E)$ = Neutron source strength at core location r, θ and energy E.

Although the adjoint importance functions used in the Byron Unit 2 analysis were based on a response function defined by the threshold neutron flux (E > 1.0 MeV), prior calculations have shown that, while the implementation of low leakage loading patterns significantly impact the magnitude and the spatial distribution of the neutron field, changes in the relative neutron energy spectrum are of second order. Thus, for a given location the ratio of dpa/ϕ (E > 1.0 MeV) is insensitive to changing core source distributions. In the application of these adjoint important functions to the Byron Unit 2 reactor, therefore, the iron displacement rates (dpa) and the neutron flux (E > 0.1 MeV) were computed on a cycle specific basis by using dpa/ϕ (E > 1.0 MeV) and ϕ (E > 0.1 MeV)/ϕ (E > 1.0 MeV) ratios from the forward analysis in conjunction with the cycle specific ϕ (E > 1.0 MeV) solutions from the individual adjoint evaluations.

The reactor core power distribution used in the plant specific adjoint calculations was taken from the fuel cycle design report for the first operating cycle of Byron Unit 2 [6]. The relative power levels in fuel assemblies that are significant contributors to the neutron exposure of the pressure vessel and surveillance capsules are summarized in Figure 6-2. For comparison purposes, the core power distribution (design basis) used in the reference forward calculation is also illustrated in Figure 6-2.

Selected results from the neutron transport analyses performed for the Byron Unit 2 reactor are provided in Tables 6-1 through 6-5. The data listed in these tables establish the means for absolute comparisons of analysis and measurement for the capsule irradiation period and provide the means to correlate dosimetry results with the corresponding neutron exposure of the pressure vessel wall.

In Table 6-1, the calculated exposure parameters [ϕ (E > 1.0 MeV), ϕ (E > 0.1 MeV), and dpa] are given at the geometric center of the two surveillance capsule positions for both the design basis and the plant specific core power distributions. The plant specific data, based on the adjoint transport analysis, are meant to establish the absolute comparison of measurement with analysis. The design basis data derived from the forward calculation are provided as a point of reference against which plant specific fluence evaluations can be compared. Similar data is given in Table 6-2 for the pressure vessel inner radius. Again, the three pertinent exposure parameters are listed for both the design basis and the cycle 1 plant specific power distributions. It is important to note that the data for the vessel inner radius were taken at the clad/base metal interface; and, thus, represent the maximum exposure levels of the vessel wall itself.

Radial gradient information for neutron flux (E > 1.0 MeV), neutron flux (E > 0.1 MeV), and iron atom displacement rate is given in Tables 6-3, 6-4, and 6-5, respectively. The data, obtained from the forward neutron transport calculation, are presented on a relative basis for each exposure parameter at several azimuthal locations. Exposure parameter distributions within the wall may be obtained by normalizing the calculated or projected exposure at the vessel inner radius to the gradient data given in Tables 6-3 through 6-5.

For example, the neutron flux (E > 1.0 MeV) at the 1/4T position on the 45° azimuth is given by:

$$\phi_{1/4T}(45°) = \phi(220.27, 45°)\ F\ (225.75, 45°)$$

where $\phi_{1/4T}(45°)$ = Projected neutron flux at the 1/4T position on the 45° azimuth

$\phi\ (220.27, 45°)$ = Projected or calculated neutron flux at the vessel inner radius on the 45° azimuth.

F (225.75, 45°) = Relative radial distribution function from Table 6-3.

Similar expressions apply for exposure parameters in terms of ϕ(E > 0.1 MeV) and dpa/sec.

The DOT calculations were carried out for a typical octant of the reactor. However, for the neutron pad arrangement in Byron Unit 2, the pad extent for all octants is not the same. For the analysis of the flux to the pressure vessel, an octant was chosen with the neutron pad extending from 32.5° to 45° (12.5°) which produces the maximum vessel flux. Other octants have neutron pads extending 22.5° or 20° which provide more shielding. For the octant with the 12.5° pad, the maximum flux to the vessel occurs near 25° and the values in the tables for the 25° angle are vessel maximum values. Exposure values for 0°, 15°, and 45° can be used for all octants; values in the tables for 25° and 35° are maximum values and only apply to octants with a 12.5° neutron pad extent.

6.3 Neutron Dosimetry

The passive neutron sensors included in the Byron Unit 2 surveillance program are listed in Table 6-6. Also given in Table 6-6 are the primary nuclear reactions and associated nuclear constants that were used in the evaluation

of the neutron energy spectrum within the capsule and the subsequent determination of the various exposure parameters of interest [ϕ (E > 1.0 Mev), ϕ (E > 0.1 MeV), dpa].

The relative locations of the neutron sensors within the capsules are shown in Figure 4-2. The iron, nickel, copper, and cobalt-aluminum monitors, in wire form, were placed in holes drilled in spacers at several axial levels within the capsules. The cadmium-shielded neptunium and uranium fission monitors were accommodated within the dosimeter block located near the center of the capsule.

The use of passive monitors such as those listed in Table 6-6 does not yield a direct measure of the energy dependent flux level at the point of interest. Rather, the activation or fission process is a measure of the integrated effect that the time- and energy-dependent neutron flux has on the target material over the course of the irradiation period. An accurate assessment of the average neutron flux level incident on the various monitors may be derived from the activation measurements only if the irradiation parameters are well known. In particular, the following variables are of interest:

- The specific activity of each monitor.
- The operating history of the reactor.
- The energy response of the monitor.
- The neutron energy spectrum at the monitor location.
- The physical characteristics of the monitor.

The specific activity of each of the neutron monitors was determined using established ASTM procedures [7 through 20]. Following sample preparation and weighing, the activity of each monitor was determined by means of a lithium-drifted germanium, Ge(Li), gamma spectrometer. The irradiation history of the Byron Unit 2 reactor during cycle 1 was obtained from NUREG-0020, "Licensed Operating Reactors Status Summary Report" for the applicable period.

The irradiation history applicable to capsule U is given in Table 6-7. Measured and saturated reaction product specific activities as well as measured full power reaction rates are listed in Table 6-8. Reaction rate values were derived using the pertinent data from Tables 6-6 and 6-7.

Values of key fast neutron exposure parameters were derived from the measured reaction rates using the FERRET least squares adjustment code [21]. The FERRET approach used the measured reaction rate data and the calculated neutron energy spectrum at the the center of the surveillance capsule as input and proceeded to adjust a priori (calculated) group fluxes to produce a best fit (in a least squares sense) to the reaction rate data. The exposure parameters along with associated uncertainties where then obtained from the adjusted spectra.

In the FERRET evaluations, a log normal least-squares algorithm weights both the a priori values and the measured data in accordance with the assigned uncertainties and correlations. In general, the measured values f are linearly related to the flux ϕ by some response matrix A:

$$f_i^{(s,\alpha)} = \sum_g A_{ig}^{(s)} \phi_g^{(\alpha)}$$

where i indexes the measured values belonging to a single data set s, g designates the energy group and α delineates spectra that may be simultaneously adjusted. For example,

$$R_i = \sum_g \sigma_{ig} \phi_g$$

relates a set of measured reaction rates R_i to a single spectrum ϕ_g by the multigroup cross section σ_{ig}. (In this case, FERRET also adjusts the cross-sections.) The lognormal approach automatically accounts for the physical constraint of positive fluxes, even with the large assigned uncertainties.

In the FERRET analysis of the dosimetry data, the continuous quantities (i.e., fluxes and cross-sections) were approximated in 53 groups. The calculated fluxes from the discrete ordinates analysis were expanded into the FERRET group structure using the SAND-II code [22]. This procedure was carried out by first expanding the a priori spectrum into the SAND-II 620 group structure using a SPLINE interpolation procedure for interpolation in regions where group boundaries do not coincide. The 620-point spectrum was then easily collapsed to the group scheme used in FERRET.

The cross-sections were also collapsed into the 53 energy-group structure using SAND II with calculated spectra (as expanded to 620 groups) as weighting functions. The cross sections were taken from the ENDF/B-V dosimetry file. Uncertainty estimates and 53 x 53 covariance matrices were constructed for each cross section. Correlations between cross sections were neglected due to data and code limitations, but are expected to be unimportant.

For each set of data or a priori values, the inverse of the corresponding relative covariance matrix M is used as a statistical weight. In some cases, as for the cross sections, a multigroup covariance matrix is used. More often, a simple parameterized form is used:

$$M_{gg'} = R_N^2 + R_g \, R_{g'} \, P_{gg'}$$

where R_N specifies an overall fractional normalization uncertainty (i.e., complete correlation) for the corresponding set of values. The fractional uncertainties R_g specify additional random uncertainties for group g that are correlated with a correlation matrix:

$$P_{gg'} = (1 - \theta) \, \delta_{gg'} + \theta \exp \left[\frac{-(g-g')^2}{2\gamma^2}\right]$$

The first term specifies purely random uncertainties while the second term describes short-range correlations over a range γ (θ specifies the strength of the latter term.)

For the a priori calculated fluxes, a short-range correlation of $\gamma = 6$ groups was used. This choice implies that neighboring groups are strongly correlated when θ is close to 1. Strong long-range correlations (or anticorrelations) were justified based on information presented by R. E. Maerker [23]. Maerker's results are closely duplicated when $\gamma = 6$. For the integral reaction rate covariances, simple normalization and random uncertainties were combined as deduced from experimental uncertainties.

Results of the FERRET evaluation of the capsule U dosimetry are given in Table 6-9. The data summarized in Table 6-9 indicated that the capsule received an integrated exposure of 3.96×10^{18} n/cm^2 (E > 1.0 MeV) with an associated uncertainty of $\pm$ 8%. Also reported are capsule exposures in terms of fluence (E > 0.1 MeV) and iron atom displacements (dpa). Summaries of the fit of the adjusted spectrum are provided in Table 6-10. In general, excellent results were achieved in the fits of the adjusted spectrum to the individual experimental reaction rates. The adjusted spectrum itself is tabulated in Table 6-11 for the FERRET 53 energy group structure.

A summary of the measured and calculated neutron exposure of capsule U is presented in Table 6-12. The agreement between calculation and measurement falls within $\pm$ 12% for all exposure parameters listed. The calculated fast neutron exposure (ϕ (E > 1.0 MeV), ϕ (E > 0.1 MeV), dpa) values agreed with the measurements to within 1-3% whereas, the thermal neutron exposure calculated for cycle 1 exceeded the measured value by 12 percent.

Neutron exposure projections at key locations on the pressure vessel inner radius are given in Table 6-13. Along with the current (1.15 EFPY) exposure derived from the capsule U measurements, projections are also provided for an exposure period of 16 EFPY and to end of vessel design life (32 EFPY). The calculated design basis exposure rates given in Table 6-2 were used to perform projections beyond the end of cycle 1.

In the calculation of exposure gradients for use in the development of heatup and cooldown curves for the Byron Unit 2 reactor coolant system, exposure projections to 16 EFPY and 32 EFPY were employed. Data based on both a fluence (E > 1.0 MeV) slope and a plant specific dpa slope through the vessel wall are provided in Table 6-14. In order to access RT_{NDT} vs. fluence trend curves, dpa equivalent fast neutron fluence levels for the 1/4T and 3/4T positions were defined by the relations

$$\phi' \text{ (1/4T)} = \phi \text{ (Surface)} \left\{ \frac{\text{dpa (1/4T)}}{\text{dpa (Surface)}} \right\}$$

$$\phi' \text{ (3/4T)} = \phi \text{ (Surface)} \left\{ \frac{\text{dpa (3/4T)}}{\text{dpa (Surface)}} \right\}$$

Using this approach results in the dpa equivalent fluence values listed in Table 6-14.

In Table 6-15 updated lead factors are listed for each of the Byron Unit 2 surveillance capsules. These data may be used as a guide in establishing future withdrawal schedules for the remaining capsules.

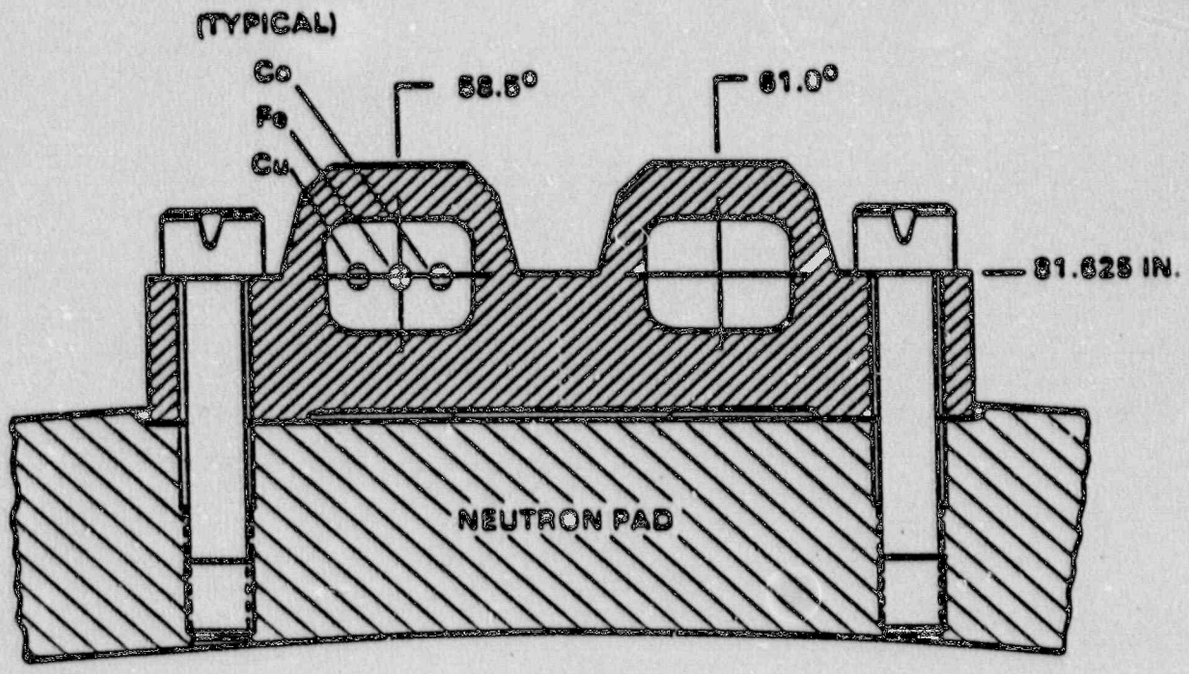

Figure 6-1. Plan View of a Dual Reactor Vessel Surveillance Capsule

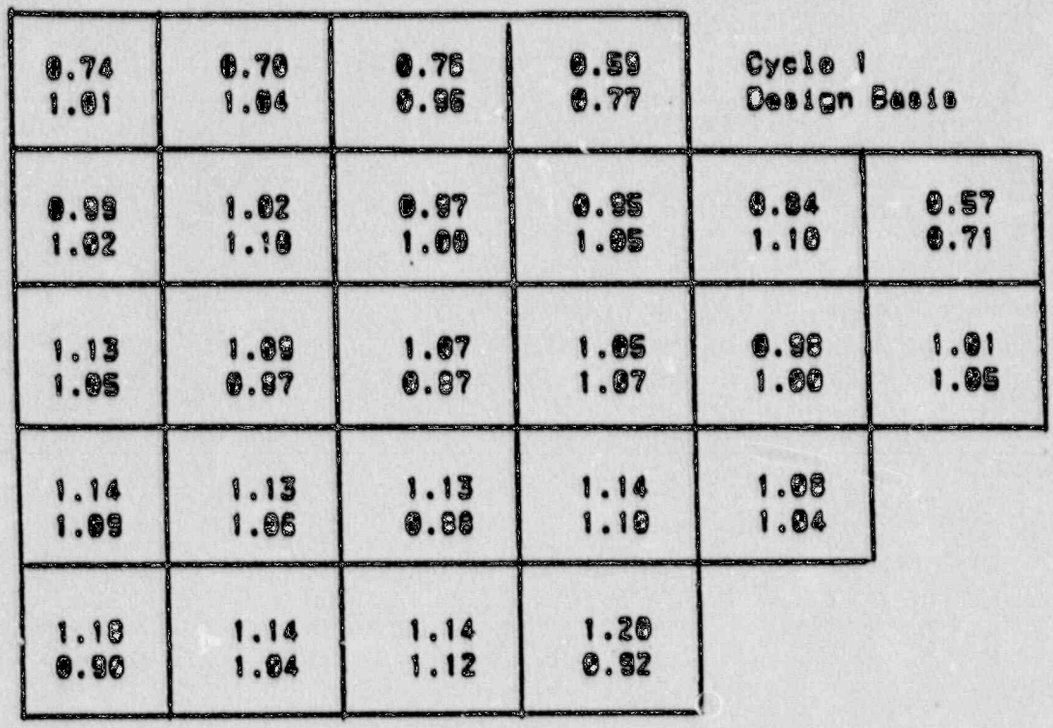

Figure 6-2. Core Power Distributions Used in Transport Calculations for Byron Unit 2

TABLE 6-1

CALCULATED FAST NEUTRON EXPOSURE PARAMETERS

AT THE SURVEILLANCE CAPSULE CENTER

	DESIGN BASIS		CYCLE 1	
	29.0°	31.5°	29.0°	31.5°
ϕ (E > 1.0 MeV) (n/cm^2-sec)	1.13×10^{11}	1.21×10^{11}	8.84×10^{10}	9.51×10^{10}
ϕ (E > 0.1 MeV) (n/cm^2-sec)	5.07×10^{11}	5.44×10^{11}	3.97×10^{11}	4.28×10^{11}
dpa/sec	2.21×10^{-10}	2.37×10^{-10}	1.73×10^{-10}	1.86×10^{-10}

TABLE 6-2

CALCULATED FAST NEUTRON EXPOSURE PARAMETERS AT
THE PRESSURE VESSEL CLAD/BASE METAL INTERFACE

DESIGN BASIS

	0°	15°	25°	35°	45°
ϕ(E> 1.0Mev) (n/cm^2-sec)	1.78×10^{10}	2.66×10^{10}	3.01×10^{10}	2.45×10^{10}	2.81×10^{10}
ϕ(E> 0.1Mev) (n/cm^2-sec)	3.70×10^{10}	5.60×10^{10}	8.22×10^{10}	6.96×10^{10}	7.04×10^{10}
dpa/sec	2.77×10^{-11}	4.12×10^{-11}	5.04×10^{-11}	4.15×10^{-11}	4.48×10^{-11}

CYCLE 1 SPECIFIC

	0°	15°	25°	35°	45°
ϕ(E> 1.0Mev) (n/cm^2-sec)	1.32×10^{10}	2.06×10^{10}	2.38×10^{10}	1.98×10^{10}	2.31×10^{10}
ϕ(E> 0.1Mev) (n/cm^2-sec)	2.74×10^{10}	4.34×10^{10}	6.50×10^{10}	5.62×10^{10}	5.79×10^{10}
dpa/sec	2.05×10^{-11}	3.19×10^{-11}	3.99×10^{-11}	3.35×10^{-11}	3.68×10^{-11}

TABLE 6-3

RELATIVE RADIAL DISTRIBUTIONS OF NEUTRON FLUX (E > 1.0 MeV)
WITHIN THE PRESSURE VESSEL WALL

Radius (cm)	0°	15°	25	35°	45°
220.27(1)	1.00	1.00	1.00	1.00	1.00
220.64	0.976	0.979	0.980	0.977	0.979
221.66	0.888	0.891	0.893	0.891	0.889
222.99	0.768	0.770	0.772	0.770	0.766
224.31	0.653	0.653	0.657	0.655	0.648
225.63	0.551	0.550	0.554	0.552	0.543
226.95	0.462	0.460	0.465	0.463	0.452
228.28	0.386	0.384	0.388	0.386	0.375
229.60	0.321	0.319	0.324	0.321	0.311
230.92	0.267	0.265	0.271	0.267	0.257
232.25	0.221	0.219	0.223	0.221	0.211
233.57	0.183	0.181	0.185	0.183	0.174
234.89	0.151	0.149	0.153	0.151	0.142
236.22	0.124	0.122	0.126	0.124	0.116
237.54	0.102	0.100	0.104	0.102	0.0945
238.86	0.0828	0.0817	0.0846	0.0835	0.0762
240.19	0.0671	0.0660	0.0689	0.0679	0.0608
241.51	0.0538	0.0522	0.0550	0.0545	0.0471
242.17(2)	0.0506	0.0488	0.0518	0.0521	0.0438

NOTES: 1) Base Metal Inner Radius
2) Base Metal Outer Radius

TABLE 6-4

RELATIVE RADIAL DISTRIBUTIONS OF NEUTRON FLUX (E > 0.1 MeV)
WITHIN THE PRESSURE VESSEL WALL

Radius (cm)	0°	15°	25°	35°	45°
220.27(1)	1.00	1.00	1.00	1.00	1.00
220.64	1.00	1.00	1.00	1.00	1.00
221.66	1.00	1.00	1.00	0.999	0.995
222.99	0.974	0.969	0.974	0.959	0.956
224.31	0.927	0.920	0.927	0.907	0.901
225.63	0.874	0.865	0.874	0.850	0.842
226.95	0.818	0.808	0.818	0.792	0.782
228.28	0.761	0.750	0.716	0.734	0.721
229.60	0.705	0.693	0.704	0.677	0.662
230.92	0.649	0.637	0.649	0.621	0.605
232.25	0.594	0.582	0.594	0.567	0.549
233.57	0.540	0.529	0.542	0.515	0.495
234.89	0.487	0.478	0.490	0.465	0.443
236.22	0.436	0.428	0.440	0.416	0.392
237.54	0.386	0.380	0.392	0.369	0.343
238.86	0.337	0.333	0.344	0.324	0.295
240.19	0.289	0.287	0.298	0.279	0.248
241.51	0.244	0.238	0.249	0.233	0.201
242.17(2)	0.233	0.226	0.237	0.223	0.186

NOTES: 1) Base Metal Inner Radius
2) Base Metal Outer Radius

TABLE 6-5

RELATIVE RADIAL DISTRIBUTIONS OF IRON DISPLACEMENT RATE (dpa)
WITHIN THE PRESSURE VESSEL WALL

Radius (cm)	0°	15°	25°	35°	45°
220.27(1)	1.00	1.00	1.00	1.00	1.00
220.64	0.984	0.981	0.984	0.983	0.984
221.66	0.912	0.909	0.917	0.921	0.915
222.99	0.815	0.812	0.826	0.833	0.821
224.31	0.722	0.719	0.737	0.747	0.730
225.63	0.638	0.634	0.656	0.668	0.647
226.95	0.563	0.559	0.584	0.597	0.572
228.28	0.497	0.493	0.519	0.533	0.506
229.60	0.439	0.435	0.462	0.475	0.447
230.92	0.387	0.383	0.410	0.423	0.394
232.25	0.341	0.338	0.364	0.376	0.347
233.57	0.300	0.297	0.322	0.334	0.305
234.89	0.263	0.261	0.285	0.295	0.266
236.22	0.230	0.228	0.250	0.260	0.231
237.54	0.199	0.198	0.218	0.227	0.199
238.86	0.171	0.170	0.189	0.196	0.169
240.19	0.145	0.144	0.161	0.167	0.140
241.51	0.121	0.119	0.135	0.139	0.113
242.17(2)	0.116	0.113	0.128	0.134	0.106

NOTES: 1) Base Metal Inner Radius
2) Base Metal Outer Radius

TABLE 6-6

NUCLEAR PARAMETERS FOR NEUTRON FLUX MONITORS

Monitor Material	Reaction of Interest	Target Weight Fraction	Response Range	Product Half-Life	Fission Yield (%)
Copper	$Cu^{63}(n,\alpha)Co^{60}$	0.6917	E > 4.7 MeV	5.272 yrs	
Iron	$Fe^{54}(n,p)Mn^{54}$	0.0582	E > 1.0 MeV	312.2 days	
Nickel	$Ni^{58}(n,p)Co^{58}$	0.6830	E > 1.0 MeV	70.90 days	
Uranium-238*	$U^{238}(n,f)Cs^{137}$	1.0	E > 0.4 MeV	30.12 yrs	5.99
Neptunium-237*	$Np^{237}(n,f)Cs^{137}$	1.0	E > 0.08 MeV	30.12 yrs	6.50
Cobalt-Aluminum*	$Co^{59}(n,\gamma)Co^{60}$	0.0015	0.4ev>E> 0.015 MeV	5.272 yrs	
Cobalt-Aluminum	$Co^{59}(n,\gamma)Co^{60}$	0.0015	E > 0.015 MeV	5.272 yrs	

*Denotes that monitor is cadmium shielded.

TABLE 6-7

IRRADIATION HISTORY OF NEUTRON SENSORS
CONTAINED IN CAPSULE U

Irradiation Period	P_j (MW_t)	$\frac{P_j}{P_{Ref.}}$	Irradiation Time (days)	Decay Time (days)
2/87	842	.247	18	809
3/87	1902	.558	31	778
4/87	1731	.508	30	748
5/87	2553	.749	31	717
6/87	1299	.381	30	687
7/87	2161	.634	31	656
8/87	854	.250	31	625
9/87	2440	.715	30	595
10/87	2684	.787	31	564
11/87	2411	.707	30	534
12/87	468	.137	31	503
1/88	2424	.711	31	472
2/88	2537	.744	29	443
3/88	2521	.739	31	412
4/88	3077	.902	30	382
5/88	2897	.849	31	351
6/88	2701	.792	30	321
7/88	2745	.805	31	290
8/88	2280	.668	31	259
9/88	1911	.560	30	229
10/88	1633	.479	31	198
11/88	1805	.529	30	168
12/88	1296	.380	31	137
1/89	931	.273	7	130

NOTE: Reference Power = 3411 MW_t

TABLE 6-8

MEASURED SENSOR ACTIVITIES AND REACTION RATES

Monitor and Axial Location	Measured Activity (dis/sec-gm)	Saturated Activity (dis/sec-gm)	Reaction Rate (RPS/NUCLEUS)
Cu-63 (n,α) Co-60			
Top	5.36×10^{4}	4.18×10^{5}	
Middle	5.02×10^{4}	3.92×10^{5}	
Average	5.19×10^{4}	4.05×10^{5}	6.18×10^{-17}
Fe-54(n,p) Mn-54			
Top	1.43×10^{6}	3.99×10^{6}	
Middle	1.33×10^{6}	3.71×10^{6}	
Bottom	1.29×10^{6}	3.60×10^{6}	
Average	1.35×10^{6}	3.77×10^{6}	6.01×10^{-15}
Ni-58 (n,p) Co-58			
Top	8.64×10^{6}	5.79×10^{7}	
Middle	7.73×10^{6}	5.18×10^{7}	
Bottom	7.80×10^{6}	5.23×10^{7}	
Average	8.06×10^{5}	5.40×10^{7}	7.71×10^{-15}
U-238 (n,f) Cs-137 (Cd)			
Middle	1.45×10^{5}	3.65×10^{6}	3.70×10^{-14}

TABLE 6-8

MEASURED SENSOR ACTIVITIES AND REACTION RATES - cont'd

Monitor and Axial Location	Measured Activity (dis/sec-gm)	Saturated Activity (dis/sec-gm)	Reaction Rate (RPS/NUCLEUS)
Np-237(n,f) Cs-137 (Cd)			
Middle	1.34×10^{6}	5.21×10^{7}	3.15×10^{-13}
Co-59 (n,γ) Co-60			
Top	1.11×10^{7}	8.66×10^{7}	
Middle	1.13×10^{7}	8.81×10^{7}	
Bottom	1.12×10^{7}	8.74×10^{7}	
Average	1.12×10^{7}	8.74×10^{7}	5.70×10^{-12}
Co-59 (n,γ) Co-60 (Cd)			
Top	5.63×10^{6}	4.39×10^{7}	
Middle	5.88×10^{6}	4.59×10^{7}	
Bottom	5.82×10^{6}	4.54×10^{7}	
Average	5.78×10^{6}	4.51×10^{7}	2.94×10^{-12}

TABLE 6-9

SUMMARY OF NEUTRON DOSIMETRY RESULTS

	TIME AVERAGED EXPOSURE RATES	
ϕ (E> 1.0 MeV) (n/cm^2-sec)	1.09×10^{11}	± 8%
ϕ (E> 0.1 MeV) (n/cm^2-sec)	4.64×10^{11}	± 15%
dpa/sec	2.05×10^{-10}	± 11%
ϕ(E< 0.414 eV) (n/cm^2-sec)	4.44×10^{10}	± 30%
	INTEGRATED CAPSULE EXPOSURE	
Φ (E> 1.0 MeV) (n/cm^2)	3.96×10^{18}	± 8%
Φ (E> 0.1 MeV) (n/cm^2)	1.69×10^{19}	± 15%
dpa	7.45×10^{-3}	± 11%
Φ (E< 0.414 eV) (n/cm^2)	1.61×10^{18}	± 30%

NOTE: Total Irradiation Time = 1.15 EFPY

TABLE 6-10

COMPARISON OF MEASURED AND FERRET CALCULATED
REACTION RATES AT THE SURVEILLANCE CAPSULE CENTER

Reaction	Measured	Adjusted Calculation	C/M
Cu-63 (n,α) Co-60	6.18×10^{-17}	6.25×10^{-17}	1.01
Fe-54 (n,p) Mn-54	6.01×10^{-15}	5.93×10^{-15}	0.99
Ni-58 (n,p) Co-58	7.71×10^{-15}	7.84×10^{-15}	1.02
U-238 (n,f) Cs-137 (Cd)	3.70×10^{-14}	3.39×10^{-14}	0.92
Np-237 (n,f) Cs-137 (Cd)	3.15×10^{-13}	3.29×10^{-13}	1.04
Co-59 (n,γ) Co-60 (Cd)	2.94×10^{-12}	2.94×10^{-12}	1.00
Co-59 (n,γ) Co-60	5.70×10^{-12}	5.70×10^{-12}	1.00

TABLE 6-11

ADJUSTED NEUTRON ENERGY SPECTRUM AT
THE SURVEILLANCE CAPSULE CENTER

Group	Energy (Mev)	Adjusted Flux (n/cm^2-sec)	Group	Energy (Mev)	Adjusted Flux (n/cm^2-sec)
1	1.73×10^{1}	8.75×10^{6}	28	9.12×10^{-3}	2.12×10^{10}
2	1.49×10^{1}	1.98×10^{7}	29	5.53×10^{-3}	2.76×10^{10}
3	1.35×10^{1}	7.67×10^{7}	30	3.36×10^{-3}	8.64×10^{9}
4	1.16×10^{1}	1.71×10^{8}	31	2.84×10^{-3}	8.28×10^{9}
5	1.00×10^{1}	3.77×10^{8}	32	2.40×10^{-3}	8.01×10^{9}
6	8.61×10^{0}	6.42×10^{8}	33	2.04×10^{-3}	2.27×10^{10}
7	7.41×10^{0}	1.47×10^{9}	34	1.23×10^{-3}	2.10×10^{10}
8	6.07×10^{0}	2.08×10^{9}	35	7.49×10^{-4}	1.96×10^{10}
9	4.97×10^{0}	4.37×10^{9}	36	4.54×10^{-4}	1.88×10^{10}
10	3.68×10^{0}	5.77×10^{9}	37	2.75×10^{-4}	2.03×10^{10}
11	2.87×10^{0}	1.21×10^{10}	38	1.67×10^{-4}	2.24×10^{10}
12	2.23×10^{0}	1.67×10^{10}	39	1.01×10^{-4}	2.18×10^{10}
13	1.74×10^{0}	2.33×10^{10}	40	6.14×10^{-5}	2.15×10^{10}
14	1.35×10^{0}	2.57×10^{10}	41	3.73×10^{-5}	2.08×10^{10}
15	1.11×10^{0}	4.67×10^{10}	42	2.26×10^{-5}	1.99×10^{10}
16	8.21×10^{-1}	5.29×10^{10}	43	1.37×10^{-5}	1.91×10^{10}
17	6.39×10^{-1}	5.46×10^{10}	44	8.32×10^{-6}	1.80×10^{10}
18	4.98×10^{-1}	3.94×10^{10}	45	5.04×10^{-6}	1.63×10^{10}
19	3.88×10^{-1}	5.52×10^{10}	46	3.06×10^{-6}	1.51×10^{10}
20	3.02×10^{-1}	5.67×10^{10}	47	1.86×10^{-6}	1.37×10^{10}
21	1.83×10^{-1}	5.61×10^{10}	48	1.13×10^{-6}	1.00×10^{10}
22	1.11×10^{-1}	4.48×10^{10}	49	6.83×10^{-7}	1.01×10^{10}
23	6.74×10^{-2}	3.12×10^{10}	50	4.14×10^{-7}	1.09×10^{10}
24	4.09×10^{-2}	1.77×10^{10}	51	2.51×10^{-7}	9.21×10^{9}
25	2.55×10^{-2}	2.33×10^{10}	52	1.52×10^{-7}	7.90×10^{9}
26	1.99×10^{-2}	1.15×10^{10}	53	9.24×10^{-8}	1.63×10^{10}
27	1.50×10^{-2}	1.47×10^{10}			

NOTE: Tabulated energy levels represent the upper energy of each group.

TABLE 6-12

COMPARISON OF CALCULATED AND MEASURED
EXPOSURE LEVELS FOR CAPSULE U

	Calculated	Measured	C/M
ϕ(E> 1.0 MeV) (n/cm^2)	3.32×10^{18}	3.96×10^{18}	0.97
ϕ(E> 0.1 MeV) (n/cm^2)	1.49×10^{19}	1.69×10^{19}	1.01
dpa	6.51×10^{-3}	7.45×10^{-3}	1.01
ϕ(E< 0.414 eV) (n/cm^2)	1.58×10^{18}	1.61×10^{18}	1.12

TABLE 6-13
NEUTRON EXPOSURE PROJECTIONS AT KEY LOCATIONS
ON THE PRESSURE VESSEL CLAD/BASE METAL INTERFACE FOR BYRON UNIT@ 2

	AZIMUTHAL ANGLE				
	0°	15°	25°(a)	35°	45°
1.15 EFPY					
ϕ(E> 1.0 MeV) (n/cm^2)	5.49×10^{17}	8.57×10^{17}	9.90×10^{17}	8.24×10^{17}	9.61×10^{17}
ϕ(E> 0.1 MeV) (n/cm^2)	1.08×10^{18}	1.71×10^{18}	2.56×10^{18}	2.21×10^{18}	2.29×10^{18}
dpa	8.24×10^{-4}	1.28×10^{-3}	1.60×10^{-3}	1.34×10^{-3}	1.47×10^{-3}
16.0 EFPY					
ϕ(E> 1.0 MeV) (n/cm^2)	8.89×10^{18}	1.33×10^{19}	1.51×10^{19}	1.23×10^{19}	1.41×10^{19}
ϕ(E> 0.1 MeV) (n/cm^2)	1.84×10^{19}	2.80×10^{19}	4.11×10^{19}	3.48×10^{19}	3.53×10^{19}
dpa	1.38×10^{-2}	2.06×10^{-2}	2.52×10^{-2}	2.08×10^{-2}	2.25×10^{-2}
32.0 EFPY					
ϕ(E> 1.0 MeV) (n/cm^2)	1.79×10^{19}	2.68×10^{19}	3.03×10^{19}	2.47×10^{19}	2.83×10^{18}
ϕ(E> 0.1 MeV) (n/cm^2)	3.71×10^{19}	5.62×10^{19}	8.26×10^{19}	7.00×10^{19}	7.08×10^{19}
dpa	2.78×10^{-2}	4.14×10^{-2}	5.07×10^{-2}	4.17×10^{-2}	4.51×10^{-2}

(a) Maximum point on the pressure vessel

TABLE 6-14

NEUTRON EXPOSURE VALUES FOR USE IN THE GENERATION OF HEATUP/COOLDOWN CURVES

16 EFPY

	NEUTRON FLUENCE (E> 1.0 MeV) SLOPE (n/cm^2)			dpa SLOPE (equivalent n/cm^2)		
	Surface	1/4 T	3/4 T	Surface	1/4 T	3/4 T
0°	8.89×10^{18}	4.83×10^{18}	1.03×10^{18}	8.89×10^{18}	5.61×10^{18}	1.95×10^{18}
15°	1.33×10^{19}	7.20×10^{18}	1.51×10^{18}	1.33×10^{19}	8.34×10^{18}	2.88×10^{18}
25°(a)	1.51×10^{19}	8.24×10^{18}	1.78×10^{18}	1.51×10^{19}	9.80×10^{18}	3.59×10^{18}
35°	1.23×10^{19}	6.69×10^{18}	1.43×10^{18}	1.23×10^{19}	8.15×10^{18}	3.05×10^{18}
45°	1.41×10^{19}	7.54×10^{18}	1.52×10^{18}	1.41×10^{19}	9.02×10^{18}	3.09×10^{18}

32 EFPY

	NEUTRON FLUENCE (E> 1.0 MeV) SLOPE (n/cm^2)			dpa SLOPE (equivalent n/cm^2)		
	Surface	1/4 T	3/4 T	Surface	1/4 T	3/4 T
0°	1.79×10^{19}	9.72×10^{18}	2.07×10^{18}	1.79×10^{19}	1.13×10^{19}	3.92×10^{18}
15°	2.68×10^{19}	1.45×10^{19}	3.05×10^{18}	2.68×10^{19}	1.69×10^{19}	5.81×10^{18}
25°(a)	3.03×10^{19}	1.66×10^{19}	3.57×10^{18}	3.03×10^{19}	1.97×10^{19}	7.21×10^{18}
35°	2.47×10^{19}	1.35×10^{19}	2.86×10^{18}	2.47×10^{19}	1.64×10^{19}	6.12×10^{18}
45°	2.83×10^{19}	1.52×10^{19}	3.06×10^{18}	2.83×10^{19}	1.81×10^{19}	6.20×10^{18}

(a) Maximum point on the pressure vessel

TABLE 6-15

UPDATED LEAD FACTORS FOR BYRON UNIT 2
SURVEILLANCE CAPSULES

Capsule	Lead Factor
U	4.00[(a)]
X	4.02
W	4.02
Z	4.02
V	3.75
Y	3.75

(a) Plant specific evaluation

SECTION 7.0
SURVEILLANCE CAPSULE REMOVAL SCHEDULE

The following removal schedule meets ASTM E185-82 and is recommended for future capsules to be removed from the Byron Unit 2 reactor vessel:

Capsule	Location (deg.)	Capsule Lead Factor	Removal Time (a)	Estimated Fluence (n/cm^2)
U	58.5	4.00	1.15 (Removed)	3.96×10^{18}
X	238.5	4.02	4.5	1.71×10^{19}(b)
V	61	3.75	8.5	3.02×10^{19}(c)
Y	241	3.75	15	5.33×10^{19}
W	121.5	4.02	Standby	-
Z	301.5	4.02	Standby	-

(a) Effective full power years from plant startup.

(b) Approximate fluence at 1/4 thickness reactor vessel wall at end of life.

(c) Approximate fluence at reactor vessel inner wall at end of life.

SECTION 8.0
REFERENCES

1. L. R. Singer, "Commonwealth Edison Company Byron Station Unit No. 2, Reactor Vessel Radiation Surveillance Program," WCAP-10398, December 1983.

2. Code of Federal Regulations, 10CFR50, Appendix G, "Fracture Toughness Requirements", and Appendix H, "Reactor Vessel Material Surveillance Program Requirements," U.S. Nuclear Regulatory Commission, Washington, D. C.

3. Regulatory Guide 1.99, Proposed Revision 2, "Radiation Damage to Reactor Vessel Materials", U.S. Nuclear Regulatory Commission, February, 1986.

4. R. G. Soltesz, R. K. Disney, J. Jedruch, and S. L. Ziegler, "Nuclear Rocket Shielding Methods, Modification, Updating and Input Data Preparation. Vol. 5--Two-Dimensional Discrete Ordinates Transport Technique", WANL-PR(LL)-034, Vol. 5, August 1970.

5. "ORNL RSCI Data Library Collection DLC-76 SAILOR Coupled Self-Shielded, 47 Neutron, 20 Gamma-Ray, P3, Cross Section Library for Light Water Reactors".

6. J. V. Alexander, et. al., "Core Physics Parameters and Plant Operations Data for the Byron Generating Station Unit 2 Cycle 1", WCAP-11136, June 1986. (Proprietary)

7. ASTM Designation E482-82, "Standard Guide for Application of Neutron Transport Methods for Reactor Vessel Surveillance", in ASTM Standards, Section 12, American Society for Testing and Materials, Philadelphia, PA, 1984.

8. ASTM Designation E560-77, "Standard Recommended Practice for Extrapolating Reactor Vessel Surveillance Dosimetry Results", in ASTM Standards, Section 12, American Society for Testing and Materials, Philadelphia, PA, 1984.

9. ASTM Designation E693-79, "Standard Practice for Characterizing Neutron Exposures in Ferritic Steels in Terms of Displacements per Atom (dpa)", in ASTM Standards, Section 12, American Society for Testing and Materials, Philadelphia, PA, 1984.

10. ASTM Designation E706-81a, "Standard Master Matrix for Light-Water Reactor Pressure Vessel Surveillance Standard", in ASTM Standards, Section 12, American Society for Testing and Materials, Philadelphia, PA, 1984.

11. ASTM Designation E853-84, "Standard Practice for Analysis and Interpretation of Light-Water Reactor Surveillance Results", in ASTM Standards, Section 12, American Society for Testing and Materials, Philadelphia, PA, 1984.

12. ASTM Designation E261-77, "Standard Method for Determining Neutron Flux, Fluence, and Spectra by Radioactivation Techniques", in ASTM Standards, Section 12, American Society for Testing and Materials, Philadelphia, PA, 1984.

13. ASTM Designation E262-77, "Standard Method for Measuring Thermal Neutron Flux by Radioactivation Techniques", in ASTM Standards, Section 12, American Society for Testing and Materials, Philadelphia, PA, 1984.

14. ASTM Designation E263-82, "Standard Method for Determining Fast-Neutron Flux Density by Radioactivation of Iron", in ASTM Standards, Section 12, American Society for Testing and Materials, Philadelphia, PA, 1984.

15. ASTM Designation E264-82, "Standard Method for Determining Fast-Neutron Flux Density by Radioactivation of Nickel", in ASTM Standards, Section 12, American Society for Testing and Materials, Philadelphia, PA, 1984.

16. ASTM Designation E481-78, "Standard Method for Measuring Neutron-Flux Density by Radioactivation of Cobalt and Silver", in ASTM Standards, Section 12, American Society for Testing and Materials, Philadelphia, PA, 1984.

17. ASTM Designation E523-82, "Standard Method for Determining Fast-Neutron Flux Density by Radioactivation of Copper", in ASTM Standards, Section 12, American Society for Testing and Materials, Philadelphia, PA, 1984.

18. ASTM Designation E704-84, "Standard Method for Measuring Reaction Rates by Radioactivation of Uranium-238", in ASTM Standards, Section 12, American Society for Testing and Materials, Philadelphia, PA, 1984.

19. ASTM Designation E705-79, "Standard Method for Measuring Fast-Neutron Flux Density by Radioactivation of Neptunium-237", in ASTM Standards, Section 12, American Society for Testing and Materials, Philadelphia, PA, 1984.

20. ASTM Designation E1005-84, "Standard Method for Application and Analysis of Radiometric Monitors for Reactor Vessel Surveillance", in ASTM Standards, Section 12, American Society for Testing and Materials, Philadelphia, PA, 1984.

21. F. A. Schmittroth, FERRET Data Analysis Core, HEDL-TME 79-40, Hanford Engineering Development Laboratory, Richland, WA, September 1979.

22. W. N. McElroy, S. Berg and T. Crocket, A Computer-Automated Iterative Method of Neutron Flux Spectra Determined by Foil Activation, AFWL-TR-67-41, Vol. I-IV, Air Force Weapons Laboratory, Kirkland AFB, NM, July 1967.

23. EPRI-NP-2188, "Development and Demonstration of an Advanced Methodology for LWR Dosimetry Applications", R. E. Maerker, et al., 1981.